Calhoun
Institutional Archive of the Naval Postgraduate School

Calhoun: The NPS Institutional Archive

DSpace Repository

Theses and Dissertations 1. Thesis and Dissertation Collection, all items

1957-06

Control-fixed lateral dynamic stability of the H-21 helicopter with free-floating vertical tail fins.

Goodspeed, Richard E.

Princeton University, 1957.

http://hdl.handle.net/10945/24647

Downloaded from NPS Archive: Calhoun

DUDLEY KNOX LIBRARY

Calhoun is the Naval Postgraduate School's public access digital repository for research materials and institutional publications created by the NPS community. Calhoun is named for Professor of Mathematics Guy K. Calhoun, NPS's first appointed -- and published -- scholarly author.

Dudley Knox Library / Naval Postgraduate School
411 Dyer Road / 1 University Circle
Monterey, California USA 93943

http://www.nps.edu/library

CONTROL-FIXED LATERAL DYNAMIC STABILITY OF THE H-21 HELICOPTER WITH FREE-FLOATING VERTICAL TAIL FINS

Richard E. Goodspeed

59

CONTROL-FIXED LATERAL DYNAMIC STABILITY OF THE H-21 HELICOPTER WITH FREE-FLOATING VERTICAL TAIL FINS

Lieutenant Richard E. Goodspeed, USN

Aeronautical Engineering Report No. 390
1 June 1957

Submitted in partial fulfillment of the requirements for the Degree of Master of Science in Engineering from Princeton University, 1957.

Thesis
G57

ACKNOWLEDGMENTS

The author wishes to express his gratitude for the contribution of time, advice, and encouragement which made the writing of this thesis possible. Those so contributing were: Professor Nikolsky, Professor Seckel, Mr. Sweeney, Mr. Durbin, and especially Mr. Joseph Goldberg.

35767

TABLE OF CONTENTS

SUBJECT	PAGE NUMBER
LIST OF TABLES	3
LIST OF FIGURES	4
SYMBOLS AND CONVENTIONS	5
SUMMARY	10
INTRODUCTION	11
DISCUSSION	12
RESULTS	24
CONCLUSIONS AND RECOMMENDATIONS	26
BIBLIOGRAPHY	28
CALCULATIONS	29
TABLES	34
FIGURES	38

LIST OF TABLES

TABLE	PAGE NUMBER
I. VALUES OF COEFFICIENTS CONTAINING K, d_1 , d_2	34
II. ROLL ANGLE RESPONSE VARIATION	36
III. ROLL RATE RESPONSE VARIATION	37

LIST OF FIGURES

FIGURE		PAGE NUMBER
1.	DRAWING OF THE H-21C	38
2.	L3 GEDA COMPUTER DIAGRAM	39
3.	THE L3 GEDA COMPUTER	40
4.	COMPUTER SOLUTION - FIXED FINS	41
5.	" " - $d_1 = -0.03$	42
6.	" " " $= -0.05$	43
7.	" " " $= -0.07$	44
8.	" " " $= -0.09$	45
9.	EFFECT OF SUSPENSION POINT ON DAMPING (ROLL ANGLE)	46
10.	EFFECT OF GEAR RATIO ON DAMPING	46
11.	EFFECT OF SUSPENSION POINT ON PERIOD (ROLL ANGLE)	47
12.	EFFECT OF SUSPENSION POINT ON DAMPING (ROLL RATE)	48
13.	EFFECT OF GEAR RATIO ON DAMPING (ROLL RATE)	48

AXIS SYSTEM AND NOTATION

The axis system used in the analysis is a body axis system, the origin of which is at the aircraft center of gravity. The X axis lies in the plane of symmetry, perpendicular to the rotor shafts, positive direction forward. The Y axis is perpendicular to the plane containing X axis and the rotor shafts, positive to the right of the helicopter. The Z axis is parallel to the rotor shafts, positive direction down.

The symbols and physical quantities used in the analysis are as follows:

GENERAL

$(\overline{\ \ })$	Bar denotes $\frac{2}{a\sigma}$ ( ).
$(\ \ )_x$	Subscript, following standard practice, denotes partial differentiation with respect to subscript quantity; $(\ \ )_x = \frac{\partial(\ )}{\partial x}$.
$(\dot{\ \ })$	Dot denotes differentiation with respect to time; $(\dot{\ \ }) = \frac{d(\ )}{d\ t}$.
D( )	Denotes differentiation with respect to non-dimensional time; $D(\ \ ) = \frac{d(\ )}{d(t/\tau)}$.

FORCES AND MOMENTS

ΣT	Sum of the thrusts of the two rotors (lbs.).
Y	Side force, positive to right (lbs.).
L, N	Rolling and yawing moments of helicopter about its C. G.; roll is positive for right side down, and yaw for nose right (ft.-lbs.).
H	Stabilizer hinge moment, positive for leading edge right (ft.-lbs.).
M_F	Rolling moment equation forcing function, i.e., rolling

	moment due to lateral cyclic stick displacement (ft.-lbs.).
Y_F	Side force equation forcing function, i.e., side force due to lateral cyclic stick displacement (lbs.).
ΣC_T	Coefficient of combined thrust of front and rear rotors. $\Sigma C_T = \frac{\Sigma T}{\rho \pi R^2 (\Omega R)^2} \doteq \frac{W}{\rho \pi R^2 (\Omega R)^2}$.
C_Y	Side force coefficient. $C_Y = \frac{Y}{\rho \pi R^2 (\Omega R)^2}$.
C_ℓ	Rolling moment coefficient. $C_\ell = \frac{L}{\rho \pi R^2 (\Omega R)^2 \ell}$.
C_n	Yawing moment coefficient. $C_n = \frac{N}{\rho \pi R^2 (\Omega R)^2 \ell}$.
C_{L_s}	Stabilizer lift coefficient.
C_{Y_F}	Side force forcing function coefficient. $C_{Y_F} = \frac{Y_F}{\rho \pi R^2 (\Omega R)^2}$.
C_{M_F}	Rolling moment forcing function coefficient. $C_{M_F} = \frac{M_F}{\rho \pi R^2 (\Omega R)^2 \ell}$.
C_h	Stabilizer hinge moment coefficient. $C_h = \frac{H}{q_t S_s c_s} \mu^2$.

PHYSICAL CHARACTERISTICS

b	Number of blades per rotor. $b = 3$.
c	Average blade chord. $c = 1.5$ ft.
c_s	Chord of vertical stabilizer. $c_s = 4.67$ ft,
d_1	Distance from aerodynamic center of vertical stabilizer to hinge line, positive for a. c. aft of hinge line, in chord lengths. $d_1 = \frac{x_{ac} - x_{HL}}{c_s} = 0.25 - \frac{x_{HL}}{c_s}$.
d_2	Distance from C. G. of vertical stabilizer to hinge line, positive for C. G. aft of hinge line, in chord lengths. $d_2 = \frac{x_{CG} - x_{HL}}{c_s} = 0.425 - \frac{x_{HL}}{c_s}$.
h_t	Distance from X axis to spanwise center of vertical stabilizer. $h_t = 5.0$ ft.

I_s	Mass moment of inertia of vertical stabilizer about vertical line through its hinge point. $I_s = 3.73$ slug ft.^{2}
I_x	Mass moment of inertia of helicopter about its X body axis. $I_x = 5400$ slug ft.^{2}
I_z	Mass moment of inertia of helicopter about its Z body axis. $I_z = 80{,}000$ slug ft.^{2}
I_{xz}	Mass product of inertia of helicopter for the X and Z body axes. $I_{xz} = 1600$ slug ft.^{2}
K	Tab gear ratio, $\frac{\delta t}{\delta s}$.
k_s	Radius of gyration of vertical stabilizer about vertical line through its hinge point. $k_s^2 = \frac{I_s}{m_s} = 1.77$ ft.^{2}
k_x	Radius of gyration of helicopter about its X body axis. $k_x^2 = \frac{I_x}{m} = 13.4$ ft.^{2}
k_z	Radius of gyration of helicopter about its Z body axis. $k_z^2 = \frac{I_z}{m} = 198.7$ ft.^{2}
ℓ	Distance between rotor shafts. $\ell = 42.3$ ft.
ℓ_o	Average distance from C. G. of helicopter to rotor shafts. $\ell_o \doteq \frac{\ell}{2} = 21.15$ ft.
ℓ_t	Distance from C. G. of helicopter to hinge point of vertical stabilizer, measured parallel to X axis. $\ell_t = 19.7$ ft.
m	Mass of helicopter. $m = 403.7$ slugs.
m_s	Mass of vertical stabilizer. $m_s = 2.11$ slugs.
q	Dynamic pressure. $q = \frac{\rho}{2} V^2$.
q_t	Dynamic pressure at tail surfaces. $q_t = \frac{\rho}{2} V_t^2$.
R	Blade radius. $R = 22.0$ ft.
S_s	Vertical stabilizer area. $S_s = 31.5$ ft.^{2}
W	Helicopter gross weight. $W = 13{,}000$ lbs.
W_s	Weight of vertical stabilizer. $W_s = 67.9$ lbs.

VELOCITIES AND ANGLES

p, r	Non-dimensionalized roll and yaw rates, respectively. $p = \frac{\ell_0 \phi}{\Omega R}$, $r = \frac{\ell_0 \dot{\psi}}{\Omega R}$.
V	Relative wind velocity, equal approximately to forward flight velocity (ft./second).
α	Angle of attack, defined as angle between relative wind and a normal to the rotor shaft (radians).
β_s	Sideslip angle of helicopter, positive for slip to right (radians).
δ_s	Stabilizer deflection angle, measured between stabilizer plane of symmetry and XZ plane, positive for leading edge right (radians).
ϕ, ψ	Roll, positive for right side down, and yaw, positive for nose to right, angles of helicopter, respectively (radians).
Ω	Angular velocity of rotor, assumed constant. $\Omega = 27.0$ radians/second.

AERODYNAMIC AND NON-DIMENSIONAL PARAMETERS

a	Slope of rotor blade two-dimensional lift curve. $a = 5.73$ per radian.
a_s	Slope of vertical stabilizer lift curve. $a_s = 1.83$ per radian.
h_s	Non-dimensional vertical stabilizer inertia parameter. $h_s = \frac{\mu_{*s}}{\mu_*^2} \left(\frac{k_s}{\ell_0}\right)^2 = 0.00086.$
h_x	Non-dimensional roll inertia parameter. $h_x = \frac{1}{a \sigma \mu_*} \left(\frac{k_x}{\ell_0}\right)^2 = 0.0153.$
h_z	Non-dimensional yaw inertia parameter. $h_z = \frac{1}{a \sigma \mu_*} \left(\frac{k_z}{\ell_0}\right)^2 = 0.227.$
h_{xz}	Non-dimensional product of inertia parameter. $h_{xz} = \frac{1}{a \sigma} \frac{I_{xz}}{\mu_* m \ell_0^2} = 0.00454.$

η_t	Tail efficiency. $\eta_t = \frac{q_t}{q} = 0.90$.
μ	Advance ratio. $\mu = \frac{V}{\Omega R}$.
μ_*	Helicopter density parameter. $\mu_* = \frac{m_s}{\rho S_s c_s} = 6.03$.
ρ	Air density (slugs/ft.^{3}).
σ	Rotor solidity. $\sigma = \frac{bc}{\pi R} = 0.065$.
τ	Non-dimensional time parameter. $\tau = \frac{m}{\rho \pi R^2 \Omega R} = 0.188$ seconds.
τ_2	Tab effectiveness. $\tau_2 = \frac{d \delta_s}{d \delta_t}$.
μ_{*_s}	Vertical stabilizer density parameter. $\mu_{*_s} = \frac{m_s}{\rho S_s c_s} = 6.03$.

SUMMARY

An analytical investigation of the effect of free floating vertical stabilizers on the lateral stability of the H-21 tandem helicopter was made for flight at sea level and 80 knots. The lateral-directional equations of motion for a tandem helicopter without free floating stabilizers were modified to account for the addition of floating fins.

The basic helicopter stability derivatives were obtained from the results of flight tests of the unmodified (fixed fin) helicopter by the manufacturer. The stability derivatives associated with the floating fins were estimated through a theoretical approach.

The fins were considered to be so mounted on the aircraft as to be mass and aerodynamically unbalanced. The aerodynamic unbalance was compensated by a geared tab. The effect on lateral stability of various combinations of tab gear ratio and mass and aerodynamic unbalance was investigated. The results were obtained by putting the modified equations on an analog computer. These results showed that, although the floating freedom of the vertical fins did not make the helicopter stable, damping of the unstable rolling mode was increased. The best combination of balance and gear ratio lengthened the time to double amplitude by 57%.

INTRODUCTION

GENERAL

The H-21 is a tandem-rotor helicopter with three-bladed, articulated rotor heads and a rotor radius of twenty-two feet. It flies at a gross weight of approximately thirteen thousand pounds, and is currently used by the armed forces of several nations of the NATO alliance. A drawing of the aircraft is shown in Figure 1.

The H-21 is unstable, but pilots feel that, compared with other helicopters, its handling characteristics are good. Its standard, fixed vertical tail fins make it an excellent test vehicle for an investigation of the possibilities of making it less unstable, or even stabilizing it, through modifications to these fins. At the time of this writing, the manufacturer has an H-21 equipped with the floating fins described in this paper, and is conducting flight tests with them. Difficulties have been encountered in this flight test program which seem to be due to aeroelasticity. Though this problem is outside the scope of this paper, it is mentioned in order to bring out the point that increasing the size or effectiveness of the fins, a logical extension of the analysis conducted here, may involve practical difficulties which are not obvious.

DESCRIPTION OF FLOATING VERTICAL STABILIZERS

The proposed free floating vertical stabilizers are NACA 0012 symmetrical airfoils of rectangular planform with a span of 6.75 feet and a chord of 4.67 feet. They are mounted on short outriggers at the rear of the fuselage, five feet above the X axis, one on each side of the helicopter. The suspension is a single hinge at the center of the span, the axis of the hinge being parallel to the span-wise direction.

The aerodynamic center of each fin is approximately at the 25% chord

point. The hinge point is varied between 0.28 c_s and 0.36 c_s in this analysis. The center of gravity has been calculated as 0.425 c_s .

The aerodynamic unbalance of the stabilizer is compensated with a trailing edge, full span tab, the leading edge of which is approximately at its hinge point which is at 80% of the stabilizer chord. The tab is so geared that a deflection of the stabilizer causes a tab deflection in the same direction, causing a restoring stabilizer hinge moment. The gear ratio, $\frac{\delta_t}{\delta_s}$, is varied between 1.5 and 2.5 in this analysis. A line drawing of the fin may be found on Page 29.

DISCUSSION

EQUATIONS OF MOTION

The lateral-directional equations of motion of the helicopter are obtained by modifying equations given in Reference 1. Equations 15 in Reference 1, modified to suit the control-fixed case are:

$$1a)\quad \left(\bar{C}_{Y_{\beta_s}} - \frac{2\mu}{a\sigma} D\right)\beta_s + \left(\frac{\bar{C}_{Y_r}}{\mu_*} - \frac{2\mu}{a\sigma}\right) D\Psi + \left[\Sigma \bar{C}_T + \left(\frac{2\mu}{a\sigma}\alpha_o + \frac{\bar{C}_{Y_p}}{\mu_*}\right) D\right]\phi = 0$$

$$1b)\quad \bar{C}_{\ell_{\beta_s}}\beta_s + \left(\frac{\bar{C}_{\ell_r}}{\mu_*} + h_{xz} D\right) D\Psi + \left(\frac{\bar{C}_{\ell_p}}{\mu_*} D - h_x D^2\right)\phi = 0$$

$$1c)\quad \bar{C}_{n_{\beta_s}}\beta_s + \left(\frac{\bar{C}_{n_r}}{\mu_*} - h_z D\right) D\Psi + \left(\frac{\bar{C}_{n_p}}{\mu_*} D + h_{xz} D^2\right)\phi = 0$$

Equations 1 are now modified to include the effects of the floating vertical stabilizers. This involves the inclusion of the additional variable, δ_s , and its coefficients in each equation, and the formulation of an additional equation; that for stabilizer hinge moments.

Equation 1a takes on a term expressing the side force due to stabilizer deflection in coefficient form,

$$2\,\bar{C}_{Y_{\delta_s}}\delta_s\ ,$$

where $\bar{C}_{Y_{\delta_s}}$ is developed as follows:

Due to stabilizer deflection, δ_s ,

$$Y = C_{L_s} q_t S_s = a_s(\delta_s - \beta_s + \tau_t K \delta_s) q_t S_s$$

$$\bar{C}_Y = \frac{2 a_s}{a \sigma} \left[\frac{\delta_s - \beta_s + \tau_t K \delta_s}{\rho \pi R^2 (\Omega R)^2} \right] q_t S_s$$

$$\bar{C}_Y = \frac{\mu^2 a_s}{a \sigma} \frac{S_s}{\pi R^2} \eta_t \beta_s + \frac{\mu^2 a_s}{a \sigma} \frac{S_s}{\pi R^2} \eta_t \delta_s (1 + \tau_t K)$$

Taking the partial derivative of $\bar{C}_Y$ with respect to δ_s , the β_s portion drops out, and

2) $$\bar{C}_{Y_{\delta_s}} = \frac{\mu^2 a_s}{a \sigma} \frac{S_s}{\pi R^2} (1 + \tau_t K) \eta_t .$$

This development has been for a single stabilizer. If the effects of airflow around the fuselage are neglected, both stabilizers may be assumed to act identically, and the total effect of stabilizer deflection on side force is equal to $2 \bar{C}_{Y_{\delta_s}} \delta_s$.

The effect of pressure variation over the stabilizer due to a deflection rate, and that of the inertia of the stabilizer and its angular acceleration are assumed to be of second order and are neglected.

Equation 1b takes on a term expressing the rolling moment due to stabilizer deflection in coefficient form,

$$2 \bar{C}_{\ell_{\delta_s}} \delta_s ,$$

where, by analogy to the $\bar{C}_{Y_{\delta_s}}$ derivation,

3) $$\bar{C}_{\ell_{\delta_s}} = \frac{h_t}{\ell} \bar{C}_{Y_{\delta_s}} .$$

Similarly, Equation 1c takes on a term expressing the yawing moment due to stabilizer deflection in coefficient form,

$$2 \bar{C}_{n_{\delta_s}} \delta_s ,$$

where, by analogy to the derivations of Equations 2 and 3,

4) $$\bar{C}_{n_{\delta_s}} = -\frac{l_t}{l}\bar{C}_{Y_{\delta_s}}$$

The effect of stabilizer deflection rate upon yawing moment may be significant, so it is included in the yawing moment equation as

$$2\bar{C}_{n_{D\delta_s}} D\delta_s$$

A general method of evaluating $C_{n_{D'\delta}}$ for a fixed wing aircraft of "average" characteristics is given in the Appendix of Reference 4, where D' is a differential operator, defined as $\frac{d}{d(Vt)}$. This method is modified to fit the parameters used in this paper, and used as an approximate method of obtaining $\bar{C}_{n_{D\delta_s}}$ for the H-21. A stabilizer deflection rate causes a change in stabilizer lift coefficient, ΔC_{L_s}. The resulting yawing moment is

$$C_n = -\frac{\Delta C_{L_s} q_t S_s l_t}{\rho \pi R^2 (.2R)^2 l}.$$

From Reference 4,

$$\Delta C_{L_s} \doteq D'\delta_s \frac{\partial C_L}{\partial D'\delta_s} + D'\delta_s \left(\frac{\partial C_L}{\partial \alpha}\right)_s \frac{\partial \alpha_t}{\partial D'\delta_s}$$

$$D' = \frac{1}{\mu \mu_* l_0} D$$

$$\Delta C_{L_s} \doteq \frac{1}{\mu \mu_* l_0}\left[D\delta_s \frac{\partial C_L}{\partial D'\delta_s} + D\delta_s \left(\frac{\partial C_L}{\partial \alpha}\right)_s \frac{\partial \alpha_t}{\partial D'\delta_s}\right].$$

Substituting, taking the derivative with respect to $D\delta_s$, and multiplying by $\frac{2}{a\sigma}$;

$$\bar{C}_{n_{D\delta_s}} \doteq -\frac{\mu}{a\sigma}\eta_t \frac{\rho S_s l_t}{l m}\left[\frac{\partial C_L}{\partial D'\delta_s} + a_s \frac{\partial \alpha_t}{\partial D'\delta_s}\right].$$

From Figure 15 of Reference 4, and considering the hinge point of the stabilizer to be at its leading edge in using this figure,

$$\frac{\partial C_L}{\partial D'\delta_s} = 3.15$$

$$\frac{\partial \alpha_t}{\partial D'\delta_s} = 1.50.$$

and

$$\bar{C}_{n_{D\delta_s}} = -\frac{\mu}{a\sigma}\eta_t \frac{\rho S_s l_t}{l m}\left[3.15 + 1.50\, a_s\right].$$

There is a similar contribution to yawing moment due to the tab deflection rate, $K\, D\, \delta_s$;

$$\bar{C}_{n_{D\delta_s}} = -\frac{\mu}{a\sigma}\eta_t \frac{\rho S_s l_t}{l m}\left[0.48 + 0.16\, a_s\right] K .$$

The total value of $\bar{C}_{n_{D\delta_s}}$ is, then

5) $$\bar{C}_{n_{D\delta_s}} = -\frac{\mu}{a\sigma}\eta_t \frac{\rho S_s l_t}{l m}\left[3.15 + 0.48K + (1.50 + 0.16K)a_s\right].$$

The stabilizer hinge moment equation is now derived. The tab, being linked to the stabilizer in a manner such that tab deflection is a linear function of the stabilizer deflection, is treated as a modifier in the various stabilizer coefficients. Tab inertia effects are neglected as being of second order.

Stabilizer hinge moments may be classified as aerodynamic and inertial.

$$H_s = H_{s_a} + H_{s_i} = 0$$

Reference 2, treating the rudder of a fixed wing aircraft, states that

$$H_{s_a} = F(\beta_s,\ \psi\ ,\ \ddot{\psi},\ \dot{\phi},\ \delta_s,\ \dot{\delta}_s),$$

with the implied conditions that the rudder be mass balanced and the center of pressure of the rudder be close to the X axis. The vertical stabilizer being considered is, however, mass unbalanced, warranting the inclusion of a function of roll angle in the above relationship, and the stabilizer center of pressure is far enough from the X axis to justify the inclusion of a function of roll rate. Including these two variables and expanding by means of partial derivatives;

$$H_{s_a} = H_{s_0} + \frac{\partial H_s}{\partial \beta_s}\Delta\beta_s + \frac{\partial H_s}{\partial \dot{\psi}}\Delta\dot{\psi} + \frac{\partial H_s}{\partial \ddot{\psi}}\Delta\ddot{\psi} + \frac{\partial H_s}{\partial \phi}\Delta\phi + \frac{\partial H_s}{\partial \dot{\phi}}\Delta\dot{\phi}$$

$$+ \frac{\partial H_s}{\partial \ddot{\phi}}\Delta\ddot{\phi} + \frac{\partial H_s}{\partial \delta_s}\Delta\delta_s + \frac{\partial H_s}{\partial \dot{\delta}_s}\Delta\dot{\delta}_s .$$

Initial conditions are straight and level, balanced flight, so that H_{s_0} and the $\triangle$'s may be dropped.

Dividing by $q_t \; S_s \; c_s$ to non-dimensionalize, and multiplying by $\frac{2}{a \, \sigma}$ for consistency;

$$\bar{C}_{h_a} = \bar{C}_{h_{\beta_s}} \beta_s + \bar{C}_{h_{\dot{\psi}}} \dot{\psi} + \bar{C}_{h_{\ddot{\psi}}} \ddot{\psi} + \bar{C}_{h_\phi} \phi + \bar{C}_{h_{\dot{\phi}}} \dot{\phi} + \bar{C}_{h_{\ddot{\phi}}} \ddot{\phi}$$

$$+ \bar{C}_{h_{\delta_s}} \delta_s + \bar{C}_{h_{\dot{\delta}_s}} \dot{\delta}_s .$$

Treating the hinge moment due to inertia;

$$H_{s_i} = - I_s \ddot{\delta}_s = - m_s \, k_s^2 \ddot{\delta}_s$$

$$\bar{C}_{h_{s_i}} = - \frac{2 \mu^2}{a \, \sigma} \frac{m_s \, k_s^2 \ddot{\delta}_s}{q_t \, S_s \, c_s} = - \frac{2 \mu^2}{a \, \sigma} \frac{m_s \, k_s^2}{q_t \, S_s \, c_s} \frac{1}{\gamma^2} D^2 \delta_s$$

$$\bar{C}_{h_{s_i}} = - \frac{4}{a \sigma \eta_t} h_s \, D^2 \, \delta_s .$$

The stabilizer hinge moment equation is now

$$6) \qquad \bar{C}_{h_{\beta_s}} \beta_s + (\bar{C}_{h_{D\psi}} + \bar{C}_{h_{D^2\psi}} D) D\psi + (\bar{C}_{h_\phi} + \bar{C}_{h_{D\phi}} D + \bar{C}_{h_{D^2\phi}} D^2) \phi$$

$$+ (\bar{C}_{h_{\delta_s}} + \bar{C}_{h_{D\delta_s}} D - \frac{4}{a \sigma \, \eta_t} h_s \, D^2) \, \delta_s = 0.$$

The equations of motion for the helicopter with floating vertical tail fins are:

$$7a) \qquad (\bar{C}_{Y_{\beta_s}} - \frac{2\mu}{a\sigma} D) \beta_s + (\frac{\bar{C}_{Y_r}}{\mu_*} - \frac{2\mu}{a\sigma}) D\psi + \left[\Sigma \bar{C}_T + \left(\frac{2\mu}{a\sigma} \alpha_0 + \frac{C_{Y_p}}{\mu_*} \right) D \right] \phi$$

$$+ 2 \, \bar{C}_{Y_{\delta_s}} \, \delta_s = 0$$

$$7b) \qquad \bar{C}_{\ell_{\beta_s}} \beta_s + \left(\frac{\bar{C}_{\ell_r}}{\mu_*} + h_{xz} D \right) D\psi + \left(\frac{\bar{C}_{\ell_p}}{\mu_*} D - h_x D^2 \right) \phi + 2 \, \bar{C}_{\ell_{\delta_s}} \, \delta_s = 0$$

$$7c) \qquad \bar{C}_{n_{\beta_s}} \beta_s + \left(\frac{\bar{C}_{n_r}}{\mu_*} - h_z D \right) D\psi + \left(\frac{\bar{C}_{n_p}}{\mu_*} D + h_{xz} D^2 \right) \phi$$

$$+ 2 \left(\bar{C}_{n_{\delta_s}} + \bar{C}_{n_{D\delta_s}} D \right) \delta_s = 0$$

$$7d) \qquad \bar{C}_{h_{\beta_s}} \beta_s + (\bar{C}_{h_{D\psi}} + \bar{C}_{h_{D^2\psi}} D) D\psi + (\bar{C}_{h_\phi} + \bar{C}_{h_{D\phi}} D + \bar{C}_{h_{D^2\phi}} D^2) \phi$$

$$+ (\bar{C}_{h_{\delta_s}} + \bar{C}_{h_{D\delta_s}} D - \frac{4}{a \sigma \, \eta_t} h_s D^2) \delta_s = 0 .$$

DEFINING STABILIZER HINGE MOMENT DERIVATIVES

The stabilizer hinge moment derivatives in Equation 7d must now be further defined.

$\bar{C}_{h_{\beta_s}}$ is the result of the aerodynamic unbalance of the stabilizer. A sideslip angle, β_s , is equivalent to an angle of attack on the vertical stabilizer, and

$$H = a_s \beta_s \, q_t \, S_s \, (d_1 \, c_s)$$

$$\bar{C}_h = \frac{2 \, a_s \beta_s \, q_t \, S_s \, d_1 \, c_s \, \mu^2}{a \, \sigma \, q \, S_s \, c_s} = 2 \, \eta_t \, \frac{a_s \, \mu^2}{a \, \sigma} d_1 \, \beta_s$$

8) $$\bar{C}_{h_{\beta_s}} = 2 \, \eta_t \, \frac{a_s \, \mu^2}{a \, \sigma} d_1$$

$\bar{C}_{h_{D\Psi}}$ is a result of the aerodynamic unbalance of the stabilizer and the effective change in vertical stabilizer angle of attack due to a yawing velocity.

$$H = a_s \, \Delta\alpha_{vt} \, q_t \, S_s \, (d_1 \, c_s)$$

$$\Delta\alpha_{vt} \doteq - \frac{\dot{\psi} \, \ell_t}{V} = - \frac{\ell_t \, D\Psi}{\tau \, V}$$

$$H = - \frac{a_s \, \ell_t \, q_t \, S_s \, d_1 \, c_s}{\tau \, V} D\Psi$$

$$\bar{C}_h = - \frac{2 \, a_s \, \ell_t \, q_t \, S_s \, d_1 \, c_s \, \mu^2}{a \, \sigma \, \tau \, V \, q \, S_s \, c_s} D\Psi = - 2 \eta_t \, \frac{a_s \mu}{a \, \sigma} \, \frac{d_1}{\mu_*} \, \frac{\ell_t}{\ell_o} D\Psi$$

9) $$\bar{C}_{h_{D\Psi}} = - 2 \, \eta_t \, \frac{a_s}{a \, \sigma} \, \frac{\mu \, d_1}{\mu_*} \, \frac{\ell_t}{\ell_o}$$

$\bar{C}_{h_{D^2\Psi}}$ is a result of the mass unbalance of the stabilizer and its linear acceleration with the helicopter's acceleration in yaw.

$$H = - m_s \, \ell_t \, \ddot{\Psi} \, (d_2 \, c_s) = - \frac{m_s \, \ell_t \, d_2 \, c_s}{\tau^2} D^2 \Psi$$

$$\bar{C}_h = - \frac{2 \, \mu^2}{a \, \sigma} \, \frac{m_s \, \ell_t \, d_2 \, c_s}{q \, S_s \, c_s} D^2 \Psi = - \frac{4}{a \, \sigma} \, \frac{\mu_s}{\mu_*^2} \, \frac{\ell_t \, c_s}{\ell_o} d_2 \, D^2 \Psi$$

10) $$\bar{C}_{h_{D^2\Psi}} = - \frac{4}{a \, \sigma} \, \frac{\mu_s}{\mu_*^2} \, \frac{\ell_t \, c_s}{\ell_o} d_2$$

$\bar{C}_{h_\phi}$ is a result of mass unbalance of the stabilizer. At any roll angle there is a component of the stabilizer weight acting to create a hinge moment.

$$H = -W_s \phi \, d_2 \, c_s$$

$$\bar{C}_h = -\frac{2\mu^2}{a\sigma}\frac{W_s d_2 c_s}{q S_s c_s}\phi = -\frac{2\mu^2}{a\sigma}\frac{m_s g d_2 c_s}{q S_s c_s}\phi = -\frac{4\mu^2}{a\sigma}\mu_{*_s}\frac{g d_2 c_s}{V^2}\phi$$

11) $$\bar{C}_{h_\phi} = -\frac{4\mu^2}{a\sigma}\mu_{*_s}\frac{g d_2 c_s}{V^2}$$

$\bar{C}_{h_{D\phi}}$ is a result of aerodynamic unbalance of the stabilizer and the effective change in angle of attack of the stabilizer due to a rolling velocity. By analogy to the derivation of $\bar{C}_{h_{D\psi}}$,

12) $$\bar{C}_{h_{D\phi}} = 2\eta_t \frac{\mu a_s}{a\sigma}\frac{d_1}{\mu_*}\frac{h_t}{l_0}.$$

$\bar{C}_{h_{D^2\phi}}$ is a result of mass unbalance of the stabilizer and is analogous to $\bar{C}_{h_{D^2\psi}}$.

13) $$\bar{C}_{h_{D^2\phi}} = \frac{4}{a\sigma}\frac{\mu_{*_s}}{\mu_*^2}\frac{h_t c_s}{l_0^2} d_2$$

$\bar{C}_{h_{\delta_s}}$ is a result of the aerodynamic unbalance of the vertical stabilizer and the sideward lift resulting from a deflection (equivalent to a change in angle of attack). Here the effect of the tab must be included, both as it affects lift and as it affects the hinge moment. Considering first the hinge moment due to the lift of the deflected stabilizer:

$$H = -a_s(\delta_s - \beta_s + \tau_2 K \delta_s) q_t S_s d_1 c_s$$

$$\bar{C}_h = -2\frac{a_s \mu^2}{a\sigma}\frac{q_t S_s d_1 c_s}{q S_s c_s}\left[\delta_s(1+\tau_2 K) - \beta_s\right]$$

$$\bar{C}_{h_{\delta_s}} = -2\eta_t \frac{a_s \mu^2}{a\sigma} d_1 (1 + \tau_2 K)$$

The additional hinge moment due to tab deflection is

$$\bar{C}_{h_{\delta_s}} = \frac{2\mu^2}{a\sigma}\frac{\partial C_h}{\partial \delta_t} K.$$

The quantity, $\frac{\partial C_h}{\partial \delta_t}$ is evaluated using a relationship derived in Reference 3:

$$\frac{\partial C_h}{\partial \delta_t} = -1.2606\, K_\phi\, K_b\, K_t\, K_c\, \eta_t.$$

As evaluated in the CALCULATIONS section of this paper,

$$\frac{\partial C_h}{\partial \delta_t} = -0.66.$$

The total value of $\bar{C}_{h_{\delta_S}}$ is, then

14) $$\bar{C}_{h_{\delta_s}} = -2\,\eta_t \frac{a_s \mu^2}{a\sigma}\, d_1 \,(1 + \tau_2 K) - 0.66 \frac{2\mu^2}{a\sigma} K.$$

$\bar{C}_{h_{D\delta_S}}$ is a result of the change in the pressure pattern over the stabilizer surface with a stabilizer deflection rate. From Reference 4,

$$C_{h_{D'\delta}} = \left(\frac{\partial C_h}{\partial D'\delta}\right)_A + \left(\frac{d C_L}{d\alpha}\right)_S \left(\frac{\partial C_h}{\partial D'\delta}\right)_B$$

$$\bar{C}_{h_{D\delta_s}} = -\frac{2\mu^2}{a\sigma V\tau} C_{h_{D\delta}} = -\frac{2\mu}{a\sigma\mu_* l_0} C_{h_{D'\delta}}$$

Figure 16 of Reference 4 gives

$$\left(\frac{\partial C_h}{\partial D'\delta}\right)_A = 2.35$$

$$\left(\frac{\partial C_h}{\partial D'\delta}\right)_B = 0.38,$$

and

$$\bar{C}_{h_{D\delta_s}} = -\frac{2\mu}{a\sigma\mu_* l_0}\,(2.35 + 0.38\, a_s).$$

There is a similar contribution to $\bar{C}_{h_{D\delta_S}}$ due to tab deflection rate, $K\, D\, \delta_S$.

$$\bar{C}_{h_{D\delta_s}} = -\frac{2\mu}{a\sigma\mu_* l_0}\,(0.8\, K + 0.14\, K a_s)$$

The total value of $\bar{C}_{h_{D\delta \cdot S}}$ is,then

15) $$\bar{C}_{h_{D\delta_s}} = -\frac{2\mu}{a\sigma\mu_* l_0}\left[2.35 + 0.8\, K + (0.38 + 0.14\, K)\, a_s\right].$$

NUMERICAL EVALUATION

In order to obtain analog computer solutions of the helicopter lateral modes, all coefficients are numerically evaluated. The stabilizer-fixed, controls-fixed, helicopter stability derivatives are evaluated using flight test data furnished by the manufacturer. The coefficients of the stabilizer hinge moment equation and the stabilizer deflection portions of the helicopter equations are evaluated by using the expressions derived in the preceding sections of this paper.

STABILIZER-FIXED, CONTROLS-FIXED STABILITY DERIVATIVES

Test conditions:

Altitude: Standard sea level

$V = 80$ knots

$\Omega = 27.0$ radians/second

Manufacturer's flight test data:

$Y_{\beta_s} = -13{,}000$ lbs./radian

$Y_{\dot{\psi}} \doteq 0$

$\Sigma T \doteq W = 13{,}000$ lb.

$\alpha_o \doteq 0$

$Y_{\dot{\phi}} \doteq 0$

$L_{\beta_s} = -22{,}500$ ft. lb./radian

$L_{\dot{\psi}} = -\ 3{,}687$ ft. lb./rad./second

$L_{\dot{\phi}} = -\ 6{,}600$ ft. lb./rad./second

$N_{\beta_s} = 20{,}000$ ft. lb./radian

$N_{\dot{\psi}} = -14{,}300$ ft. lb./rad./second

$N_{\dot{\phi}} = 2{,}200$ ft. lb./rad./second

Non-dimensional stability derivatives:

$\bar{C}_{Y_{\beta_s}} = -0.0546$

$\bar{C}_{Y_r} \doteq 0$

$\Sigma\bar{C}_T \doteq 0.0546$

$\bar{C}_{Y_p} \doteq 0$

$\bar{C}_{\ell_{\beta_s}} = -0.002245$

$\bar{C}_{\ell_r} = -0.0103$

$\bar{C}_{\ell_p} = -0.01882$

$\bar{C}_{n_{\beta_s}} = 0.002245$

$\bar{C}_{n_r} = -0.0398$

$\bar{C}_{n_p} = 0.00614$

STABILIZER-FREE DERIVATIVES

$\bar{C}_{Y_{\delta_s}} = 0.00475 + 0.00189\ K$

$\bar{C}_{\ell_{\delta_s}} = 0.000562 + 0.000224\ K$

$\bar{C}_{n_{\delta_s}} = -0.00221 - 0.000885\ K$

$\bar{C}_{n_{D\delta_s}} = -0.00028 - 0.0000368\ K$

$\bar{C}_{h_{\beta_s}} = 0.459\ d_1$

$\bar{C}_{h_{D\psi}} = -0.3575\ d_1$

$\bar{C}_{h_{D^2\psi}} = -0.479\ d_2$

$\bar{C}_{h_\phi} = -0.0276\ d_2$

$\bar{C}_{h_{D\phi}} = 0.0906\ d_1$

$\bar{C}_{h_{D^2\phi}} = 0.1217\ d_2$

$\bar{C}_{h_{\delta_s}} = (-0.458 - 0.183\ K)\ d_1 - 0.183\ K$

$\bar{C}_{h_{D\delta_s}} = -0.0334 - 0.0116\ K$

OTHER NON-DIMENSIONAL COEFFICIENTS

$$\frac{2\mu}{a\sigma} = 1.22$$

$$\frac{4\ h_s}{a\ \sigma\ \eta_t} = 0.01029$$

NUMERICAL EQUATIONS FOR FLIGHT AT SEA LEVEL AND 80 KNOTS

16a) $$(-0.0546-1.22D)\beta_s - 1.22D\Psi + 0.0546\Phi + (0.0095 + 0.00378K)\delta_s = 0$$

16b) $$-0.002245\beta_s + (-0.001961 + 0.00454D)D\Psi + (-0.00351D - 0.0153D^2)\phi$$

$$+ (0.001124 + 0.000448K)\delta_s = 0$$

16c) $$0.0020\beta_s + (-0.0076 - 0.227D)D\Psi + (0.00117D + 0.00454D^2)\phi$$
$$+ [-0.00442 - 0.00177K - (0.00056 + 0.0000736K)D]\delta_s = 0$$

16d) $$0.459d_1\beta_s + (-0.3575d_1 - 0.479d_2D)D\Psi + (-0.0276d_2 + 0.0906d_1D + 0.1217d_2D^2)\phi$$

$$+ [(-0.458 - 0.183K)d_1 - 0.183K + (-0.0334 - 0.0116K)D - 0.01029D^2)\delta_s = 0$$

FORCING FUNCTIONS

To obtain results for different combinations of gear ratio and suspension point which may be compared in a straightforward manner, a control input is used to provide forcing functions in the computer setup. The control input used in this analysis is a one inch right displacement of the cyclic stick, displace and hold.

Manufacturer's data indicate that, at 80 knots and sea level, the rolling moment produced by lateral cyclic control is 119,880 ft. lb. per radian. The control linkage gives 0.015 radians per inch of stick deflection. Therefore, the applied rolling moment for one inch of lateral cyclic stick displacement is 1,798 ft. lb. Non-dimensionalizing and multiplying by $\frac{2}{a\sigma}$ for consistency,

$$\bar{C}_{M_F} = 0.0001798.$$

This becomes the forcing function on the right side of Equation 16b, with a minus sign.

The manufacturer also indicates that right cyclic stick displacement produces a side force. This is the gross weight times the swash plate displacement in radians, or 0.015 W per inch of lateral cyclic stick displacement. Non-dimensionalizing and multiplying by $\frac{2}{a\sigma}$ for consistency,

$$\bar{C}_{Y_F} = 0.000818.$$

This becomes the forcing function on the right side of Equation 16a, with a minus sign.

TABULATION OF COEFFICIENTS

All coefficients in Equations 16 which contain d_1 and d_2 change in value during the investigation, as the suspension point is changed. Similarly, coefficients containing K change when the gear ratio is changed. In order to make the equations more adaptable to computer solution, they are rewritten as

17a) $$-1.22\,D\beta_s = 0.0546\,\beta_s + 1.22\,D\psi - 0.0546\,\phi - C_1\,\delta_s - 0.000818$$

17b) $$-0.0153\,D^2\phi = 0.002245\,\beta_s - 0.00454\,D^2\psi + 0.001961\,D\psi + 0.00351\,D\phi - C_2\,\delta_s - 0.0001798$$

17c) $$-0.227\,D^2\psi = -0.0020\,\beta_s + 0.0076\,D\psi - 0.00454\,D^2\phi - 0.00117\,D\phi + C_3\,D\,\delta_s + C_4\,\delta_s$$

17d) $$-0.1985\,D^2\,\delta_s = -C_5\,\beta_s + C_6\,D^2\psi + C_7\,D\psi - C_8\,D^2\phi - C_9\,D\phi + C_{10}\,\phi + C_{11}\,D\,\delta_s + C_{12}\,\delta_s$$

where

$C_1 = 0.00950 + 0.00378\ K$

$C_2 = 0.001124 + 0.000448\ K$

$C_3 = 0.00056 + 0.0000736\ K$

$C_4 = 0.00442 + 0.00177\ K$

$C_5 = 0.459\ d_1$

$C_6 = 0.479\ d_2$

$C_7 = 0.3575\ d_1$

$C_8 = 0.1217\ d_2$

$C_9 = 0.0906\ d_1$

$C_{10} = 0.0276\ d_2$

$C_{11} = 0.0334 + 0.0116\ K$

$C_{12} = (0.458 + 0.183\ K)\ d_1 + 0.183\ K$

and the values of these constants are tabulated in Table I.

COMPUTER SOLUTION

Equations 17 are now set up on the L3 GEDA analog computer. The computer diagram and potentiometer settings are shown in Figure 2. A photograph of the computer is shown in Figure 3, though it is to be noted that the problem set up on the problem board in the figure is not the one treated here. Four computer runs are made for each gear ratio, each of the four being for a different vertical stabilizer suspension point. The quantities ϕ, $D\phi$, $D\psi$, and δ_s are recorded on the Sanborn recorder (left foreground of Figure 3). The recorded computer results are shown in Figures 4 - 8.

RESULTS

ROLL ANGLE

The results of this analysis can best be interpreted by observing the roll angle traces from the Sanborn recorder. Figure 4 shows that the rolling motion of the helicopter with fixed fins is a straight, oscillatory divergence, with a period of approximately 7.3 seconds and time to double amplitude of approximately 7 seconds. Figures 5 - 8 show that the major result of adding the floating fin degree of freedom is to increase damping. A secondary result is a slight reduction in period. A new long period mode has also been introduced into the roll motion. A separate computer run was made, recording only roll angle, with the record scaled down to show up this long period mode to best advantage. The computer overloaded after seven of the seven-second oscillations, but enough of a record was obtained to show that the new mode is a pure convergence, reaching steady state in approximately four cycles of the seven-second mode. The seven-second mode continued to oscillate divergently about the steady-state value of the pure convergent mode.

Figures 9 and 10 and Table II show the variation in damping with suspension point and with tab gear ratio. It is evident from these figures that the optimum combination of aerodynamic unbalance and gear ratio is not in the range examined. An additional series of computer runs (records of which are not shown here) shows that even further improvement of the damping is effected by moving the suspension point farther forward (bringing the absolute value of d_1 closer to zero), and by decreasing the gear ratio. Unfortunately, a crowded computer schedule and other factors combined to prevent detailed analysis of the additional computer runs or continuation of the investigation until the optimum combination of suspension point and gear ratio were found.

In the area investigated, the best combination of suspension point ($d_1 = -0.03$) and gear ratio ($K = 1.5$) produced an increase in time to double amplitude for the roll angle oscillation of approximately 57%

Figure 11 shows the variation in period of the roll angle oscillation with suspension point and gear ratio. It is seen that, at K equal to 1.5, and d_1 equal to -0.03 (the optimum damping combination of those tested), the period is reduced by approximately 2.5%. This is not significant, and is smaller than the limits of accuracy of the Sanborn recorder record and methods for measurement of quantities recorded on it.

ROLL RATE

The effect of the addition of the floating degree of freedom to the helicopter on the roll rate modes can be seen in Figures 4 - 8 to be mainly that of additional damping, plus a small decrease in period, as in the roll angle motions.

Figure 12 shows again that the optimum combination of suspension point and gear ratio was not included in the test runs.

A comparison of Tables II and III indicates that, within the limits of accuracy of the record and record analysis, the effect upon the period

of the roll rate is the same as upon that of the roll angle.

YAW RATE

The yaw rate records in Figures 4 - 8 were made in order to disclose unusual variations in the yaw rate, if any. The problem solution did not run long enough to permit a more or less quantitative analysis of this motion. Qualitatively, it can be seen that the addition of floating fins gives a higher mean yaw rate and better damping of the oscillations, while shortening the period slightly.

STABILIZER DEFLECTION

As in the case of yaw rate, the stabilizer deflection was recorded in an effort to locate any irregularities which might show up in this degree of freedom. The only irregularity to be noted is an expected one; the heavily damped, very short period oscillation which is seen at the beginning of each run. Although adjustment of the Sanborn recorder precludes any positive statements about the magnitudes of the stabilizer deflection, it is safe to say that, over the time interval studied, they are not very large, and appear to tend to remain well within the range of mechanical possibility.

CONCLUSIONS AND RECOMMENDATIONS

The addition of a free floating degree of freedom to the vertical stabilizers of the H-21 helicopter theoretically produces more favorable damping characteristics of the lateral oscillations. Varying the aerodynamic unbalance of the stabilizers varies the amount of improvement in damping attainable, as does varying the gear ratio of the balancing tab.

Though the combinations of aerodynamic unbalance and balancing tab gear ratio tested do not contribute enough to stability to make the damping positive, the use of the optimum combination in conjunction with other stability-improving devices could conceivably bring about lateral dynamic stability.

In the absence of other stability-improving devices, it is doubtful that any combination of aerodynamic unbalance and balancing tab gear ratio could bring about positive damping of the lateral dynamic modes. However, further investigation of the areas not investigated is recommended, in order that the optimum combination might be found. The root-locus method could be used here to great advantage.

The analysis was conducted for one flight speed, and its applicability is thereby limited. It is recommended that several other flight speeds also be investigated in an effort to determine whether or not the floating vertical stabilizer has a negative effect on lateral stability at other speeds.

The low aspect ratio and small area of the stabilizers considered lead to a recommendation that the same problem be investigated using stabilizers of increased span, thus increasing area and aspect ratio and making the stabilizers more effective.

REFERENCES

1. Seckel, Edward, and Graziani, Gerald: Tandem Helicopter Lateral Stability and Control. Princeton University Aeronautical Engineering Laboratory Report No. 363, October 1956.

2. Perkins, Courtland D., and Hage, Robert E.: *Airplane Performance, Stability, and Control*. John Wiley and Sons, New York, 1949.

3. Crandall, Stewart M., and Murray, Harry E.: Analysis of Available Data on the Effects of Tabs on Control-surface Hinge Moments. NACA TN 1049, May 1946.

4. Jones, Robert T., and Cohen, Doris: An Analysis of the Stability of an Airplane with Free Controls. NACA TR 709, August 1940.

CALCULATIONS

$\frac{\partial C_h}{\partial \delta_t}$

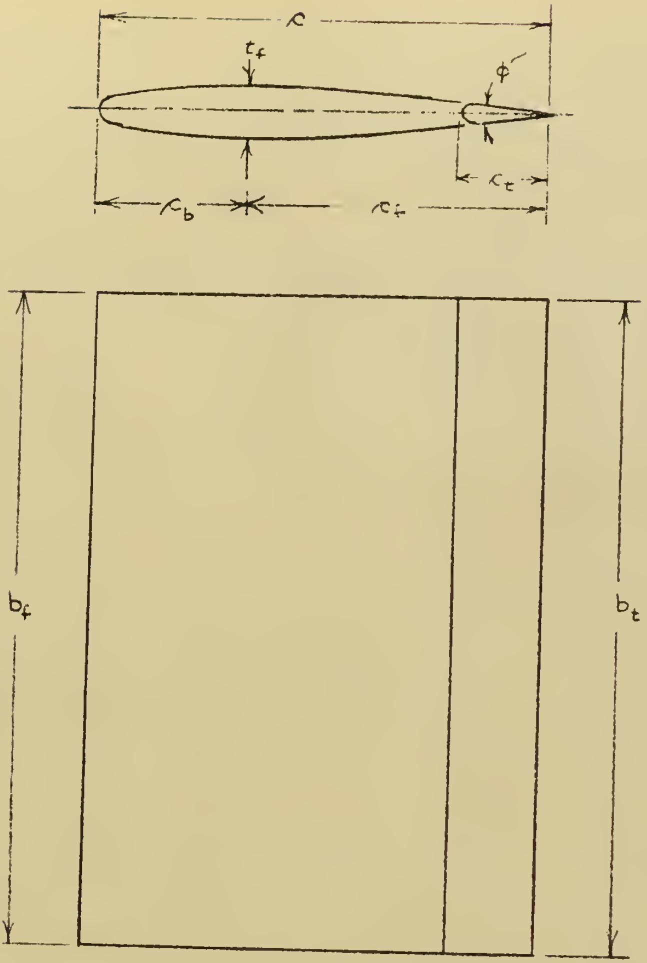

$$\frac{\partial C_h}{\partial \delta_t} = -1.2606\, K_\phi\, K_b\, K_t\, K_c\, \eta_t$$

$$K_\phi = 1.3 - 0.026\,\phi \qquad \phi = 15^\circ$$

$$K_\phi = 1.3 - 0.39 = 0.9$$

$$K_t = \frac{b_t}{b_f}\left(\frac{c_f'}{c_f}\right)^2 = 1.0$$

$$K_c = \left(\frac{c_t}{c_f}\right)^{0.7} + 0.51\,\frac{c_f}{c}$$

Note: Drawing is approximately to scale. Measurements made on actual blueprints.

$c_t = 1.3$ inches $\qquad\qquad \bar{c} = 56.0$ inches

$$c_f = (1 - 0.25 + d_1)\ 56 = (0.75 + d_1)\ 56$$

$$K_c = 0.326\ (0.75 + d_1)^{-0.7} + 0.51\ (0.75 + d_1)$$

$$K_b = 1 - 0.85 \left[\left(\frac{c_b}{c_f}\right)^2 - \left(\frac{t_f}{2c_f}\right)^2 \right] \qquad c_b = (0.25 - d_1)\ 56,$$

$$t_f \doteq 6.8 \text{ inches}$$

Evaluating the product of K_b and K_c with the hinge point of the stabilizer at its extremes,

at $d_1 = -0.03$, $K_bK_c = 0.687$

and at $d_1 = -0.09$, $K_bK_c = 0.604$.

For simplicity, the mean will be used for all hinge points, i.e.,

$$K_bK_c = 0.646.$$

Then,

$$\frac{\partial C_h}{\partial \delta t} = (-1.2606)\ (0.9)\ (0.646)\ (0.90) = -0.66.$$

NON-DIMENSIONALIZING MANUFACTURER'S DATA

$$\bar{C}_{Y_{\beta_s}} = \frac{2}{a\sigma} \frac{Y_{\beta_s}}{\rho\pi R^2(\Omega R)^2}$$

$$\frac{2}{a\sigma} = \frac{2}{(5.75)(0.065)} = 5.36$$

$$\rho\pi R^2 = (0.00238)(1520) = 3.62$$

$$(\Omega R)^2 = [(27.0)(22.0)]^2 = 353{,}000$$

$$\rho\pi R^2(\Omega R)^2 = 1{,}228{,}000$$

$$\bar{C}_{Y_{\beta_s}} = 5.36 \frac{-13{,}000}{1{,}228{,}000} = -0.0546$$

$$\Sigma \bar{C}_T \doteq \frac{2}{a\sigma} \frac{W}{\rho\pi R^2(\Omega R)^2} = 5.36 \frac{13{,}000}{(3.62)(353{,}000)} = 0.0546$$

$$\bar{C}_{\ell_{\beta_s}} = \frac{2}{a\sigma} \frac{L_{\beta_s}}{\rho\pi R^2(\Omega R)^2\ell}$$

$$\rho\pi R^2(\Omega R)^2\ell = (1{,}228{,}000)(42.3) = 54.05 \times 10^6$$

$$\bar{C}_{\ell_{\beta_s}} = 5.36 \frac{-22{,}500}{54.04 \times 10^6} = -0.002245$$

$$\bar{C}_{\ell_r} = \frac{\Omega R}{\ell_0} \frac{2}{a\sigma} \frac{L_{\dot\psi}}{\rho\pi R^2(\Omega R)^2\ell}$$

$$\frac{\Omega R}{\ell_o} = \frac{(27)(22)}{21.15} = 29.15$$

$$\bar{C}_{\ell_r} = (29.15)(5.36)\ \frac{-3687}{54.04 \times 10^6} = -0.0103$$

$$\bar{C}_{\ell_p} = \frac{\Omega R}{\ell_o}\ \frac{2}{a\sigma}\ \frac{L_{\dot{\phi}}}{\rho \pi R^2 (\Omega R)^2 \ell} = (29.15)(5.36)\ \frac{-6600}{54.04 \times 10^6} = -0.01882$$

$$\bar{C}_{n_{\beta_s}} = \frac{2}{a\sigma}\ \frac{N_{\beta_s}}{\rho \pi R^2 (\Omega R)^2 \ell} = 5.36\ \frac{20{,}000}{54.04 \times 10^6} = 0.002245$$

$$\bar{C}_{n_r} = \frac{\Omega R}{\ell_o}\ \frac{2}{a\sigma}\ \frac{N_{\dot{\psi}}}{\rho \pi R^2 (\Omega R)^2 \ell} = (29.15)(5.36)\ \frac{-14{,}300}{54.04 \times 10^6} = -0.0398$$

$$\bar{C}_{n_p} = \frac{\Omega R}{\ell_o}\ \frac{2}{a\sigma}\ \frac{N_{\dot{\phi}}}{\rho \pi R^2 (\Omega R)^2 \ell} = (29.15)(5.36)\ \frac{2200}{54.04 \times 10^6} = 0.00614$$

EVALUATING DERIVED, STABILIZER-FREE DERIVATIVES

$$\bar{C}_{Y_{\delta_s}} = \frac{\mu^2\ a_s\ S_s}{a\ \sigma\ \pi\ R^2}\ (1 + \tau_2\ K)\ \eta_t$$

$$\frac{a_s}{a\sigma} = \frac{1.83}{(5.73)(0.065)} = 4.92$$

$$\frac{S_s}{\pi R^2} = \frac{31.5}{1520} = 0.0207$$

$$\mu = \frac{V}{\Omega R}$$

For $V = 135$ ft./sec., $\Omega = 27.0$ rad./sec.,

$$\mu = \frac{135}{(27)(22)} = 0.2275,\ \mu^2 = 0.0518$$

$$\mu^2\ \frac{a_s}{a\sigma}\ \frac{S_s}{\pi R^2}\ \eta_t = (0.0518)(4.92)(0.0207)(0.90) = 0.00475$$

From Figure 5-33 of Reference 2,

$\tau_2 = 0.40.$

$$\bar{C}_{Y_{\delta_s}} = (0.00475)(1 + 0.4\ K) = 0.00475 + 0.00189\ K$$

$$\bar{C}_{\ell_{\delta_s}} = \frac{h_t}{\ell}\ \bar{C}_{M_{\delta_s}} = \frac{5.0}{42.3}\ \bar{C}_{Y_{\delta_s}} = 0.000562 + 0.000224\ K$$

$$\bar{C}_{n_{\delta_s}} = -\ \frac{\ell_t}{\ell}\ \bar{C}_{Y_{\delta_s}} = -\ \frac{19.7}{42.3}\ \bar{C}_{Y_{\delta_s}} = -\ 0.00221 - 0.000885\ K$$

$$\bar{C}_{n_{D\delta_s}} = -\ \frac{\mu}{a\sigma}\ \eta_t\ \frac{\rho\ S_s\ \ell_t}{\ell\ \mathrm{III}}\ \left[3.15 + 0.48\ K + (1.5 + 0.16\ K)\ a_s\right]$$

$$\bar{C}_{n_{D\delta_s}} = -(0.2275)(2.68)(0.90)\frac{(0.00238)(31.5)(19.7)}{(42.3)(403.7)}\left[\qquad\qquad\right]$$

$$\bar{C}_{n_{D\delta_s}} = -0.00280 - 0.0000368\ K$$

$$\bar{C}_{h\beta_s} = 2\eta_t\frac{\mu^2 a_s}{a\sigma}d_1 = (2)(0.90)(4.92)(0.0518)\ d_1 = 0.459\ d_1$$

$$\bar{C}_{h_{D\psi}} = -2\eta_t\frac{\mu a_s}{a\sigma}\frac{d_1}{\mu_*}\frac{\ell_t}{\ell_o} = -\frac{(0.2275)(8.86)}{(5.27)}\frac{19.7}{21.15}d_1 = -0.3575\ d_1$$

$$\bar{C}_{h_{D2\psi}} = -\frac{4}{a\sigma}\frac{\mu_{*s}}{\mu_*^2}\frac{\ell_t c_s}{\ell_o^2}d_2 = -10.72\frac{6.03}{(5.27)^2}\frac{(19.7)(4.67)}{18{,}200}d_2$$

$$\bar{C}_{h_{D^2\psi}} = -0.479\ d_2$$

$$\bar{C}_{h\phi} = -\frac{4\mu^2}{a\sigma}\frac{\mu_{*s}\ g\ c_s}{V^2}d_2 = -(10.720)(0.0518)(6.03)\frac{(32.2)(4.67)}{18{,}200}d_2$$

$$\bar{C}_{h\phi} = -0.0276\ d_2$$

$$\bar{C}_{h_{D\phi}} = 2\eta_t\frac{\mu a_s}{a\sigma}\frac{d_1}{\mu_*}\frac{h_t}{\ell_o} = -\frac{h_t}{\ell_t}\bar{C}_{h_{D\psi}} = \frac{5.0}{19.7}0.3575\ d_1 = 0.0906\ d_1$$

$$\bar{C}_{h_{D^2\phi}} = \frac{\mu_{*s}4}{\mu_*^2 a\sigma}\frac{h_t c_s}{\ell_o^2}d_2 = -\frac{h_t}{\ell_t}\bar{C}_{h_{D^2\psi}} = \frac{5.0}{19.7}0.479\ d_2 = 0.1217\ d_2$$

$$\bar{C}_{h_{\delta_s}} = -2\eta_t\frac{\mu^2 a_s}{a\sigma}d_1(1+\tau_2 K) - 0.66\frac{2\mu^2}{a\sigma}K$$

$$\bar{C}_{h_{\delta_s}} = -(1.8)(4.92)(0.0517)(1+0.4\ K)\ d_1 - (3.54)(0.0517)\ K$$

$$\bar{C}_{h_{\delta_s}} = (-0.458 - 0.183\ K)\ d_1 - 0.183\ K$$

$$\bar{C}_{h_{D\delta_s}} = -\frac{2\mu}{a\sigma\ \mu_*\ \ell_o}\left[2.35 + 0.8\ K + (0.38 + 0.14\ K)\ a_s\right]$$

$$\bar{C}_{h_{D\delta_s}} = -\frac{(5.36)(0.2275)}{(5.27)(21.15)}\left[2.35 + 0.8\ K + (0.38 + 0.14\ K)(1.83)\right]$$

$$\bar{C}_{h_{D\delta_s}} = -0.01098\left[2.235 + 0.8\ K + 0.695 + 0.256\ K\right] = -0.0334 - 0.0116\ K$$

NON-DIMENSIONALIZING FORCING FUNCTIONS

M_F = (119,880 Ft. Lb./Radian) x (Control Displacement in Inches) x (0.015 Radians per Inch of Displacement)

Control Displacement = 1 Inch

M_F = 1,798 Ft. Lb.

$$\bar{C}_{M_F} = \frac{2}{a\sigma}\frac{M_F}{\rho\pi R^2(\Omega R)^2\ell} = 5.36\frac{1{,}798}{54.05\times10^6} = 0.0001798$$

Y_F = (W) (0.015) = (13,000) (0.015) = 195 Lb.

$$\bar{C}_{Y_F} = \frac{2}{a\,\sigma}\,\frac{Y_F}{\rho\,\pi\,R^2(\Omega R)^2} = 5.36\,\frac{195}{(3.62)\,(353{,}000)} = 0.000818$$

TABLE I

VALUES OF COEFFICIENTS CONTAINING K, d_1, d_2

COEFFICIENT	K	d_1	d_2	VALUE
C_1	1.5			0.01518
	2.0			0.01703
	2.5			0.0189
C_2	1.5			0.001797
	2.0			0.00202
	2.5			0.00226
C_3	1.5			0.000671
	2.0			0.000706
	2.5			0.000745
C_4	1.5			0.00706
	2.0			0.00796
	2.5			0.00885
C_5		-0.03		-0.0138
		-0.05		-0.0229
		-0.07		-0.0321
		-0.09		-0.0413
C_6		-0.03	0.145	0.0694
		-0.05	0.125	0.0598
		-0.07	0.105	0.0504
		-0.09	0.085	0.0407
C_7		-0.03		-0.0107
		-0.05		-0.01785
		-0.07		-0.0250
		-0.09		-0.0322
C_8		-0.03	0.145	0.01767
		-0.05	0.125	0.01521
		-0.07	0.105	0.0128
		-0.09	0.085	0.01036
C_9		-0.03		-0.00272
		-0.05		-0.00452
		-0.07		-0.00634
		-0.09		-0.00816
C_{10}		-0.03	0.145	0.00400
		-0.05	0.125	0.00346
		-0.07	0.105	0.00291
		-0.09	0.085	0.00235

TABLE I (CONTINUED)

VALUES OF COEFFICIENTS CONTAINING K, d_1, d_2

COEFFICIENT	K	d_1	d_2	VALUE
C_{11}	1.5			0.0509
	2.0			0.0567
	2.5			0.0624
C_{12}	1.5	-0.03		0.253
		-0.05		0.238
		-0.07		0.224
		-0.09		0.209
	2.0	-0.03		0.342
		-0.05		0.325
		-0.07		0.309
		-0.09		0.292
	2.5	-0.03		0.431
		-0.05		0.413
		-0.07		0.395
		-0.09		0.375

TABLE II

ROLL ANGLE RESPONSE VARIATION

d_1	K	Period					Time to Double Amplitude				
		Upper Peaks		Lower Peaks		Ave.	Upper Peaks		Lower Peaks		Ave.
		ndt	sec.	ndt	sec.	sec.	ndt	sec.	ndt	sec.	sec.
-0.03	1.5	36.6	6.88	39.0	7.34	7.11	49.6	9.31	67.2	12.62	10.96
	2.0	37.6	7.06	39.0	7.34	7.20	44.0	8.26	63.4	11.91	10.08
	2.5	38.4	7.22	38.6	7.26	7.24	42.8	8.04	58.0	10.90	9.47
-0.05	1.5	36.0	6.76	38.2	7.18	6.97	46.4	8.71	70.4	13.22	10.96
	2.0	36.8	6.91	38.2	7.18	7.04	39.4	7.41	59.2	11.13	9.27
	2.5	37.4	7.03	37.8	7.10	7.06	40.0	7.52	54.8	10.30	8.91
-0.07	1.5	34.4	6.46	37.4	7.04	6.75	40.2	7.55	73.2	13.78	10.66
	2.0	35.8	6.73	37.2	6.99	6.86	37.4	7.04	60.6	11.40	9.22
	2.5	36.4	6.84	38.0	7.15	7.00	39.4	7.41	54.4	10.22	8.82
-0.09	1.5	34.6	6.51	36.2	6.80	6.66	39.0	7.34	72.4	13.60	10.47
	2.0	35.0	6.58	36.4	6.84	6.71	40.2	7.55	58.0	10.90	9.22
	2.5	35.6	6.69	37.2	6.99	6.84	36.0	6.76	55.6	10.46	8.61
Fixed Fin		40.4	7.10	39.6	7.45	7.28	29.8	5.60	44.2	8.31	6.96

Note: Upper peak values of period measured between first and second maxima.

Lower peak values of period measured between first and second minima.

Upper peak values of time to double amplitude measured from amplitude at first maximum.

Lower peak values of time to double amplitude measured from amplitude at first minimum.

ndt signifies non-dimensional time, t/τ, as used on the computer and in the analysis.

TABLE III

ROLL RATE RESPONSE VARIATION

d_1	K	Period					Time to Double Amplitude				
		Upper Peaks		Lower Peaks		Ave.	Upper Peaks		Lower Peaks		Ave.
		ndt	sec.	ndt	sec.	sec.	ndt	sec.	ndt	sec.	sec.
-0.03	1.5	37.6	7.06	37.6	7.06	7.06	73.6	13.82	69.4	13.03	13.42
	2.0	37.4	7.03	37.0	6.95	6.99	67.4	12.67	62.4	11.72	12.20
	2.5	37.2	6.99	37.6	7.06	7.02	57.6	10.83	58.4	10.98	10.90
-0.05	1.5	36.4	6.84	36.2	6.80	6.82	68.6	12.90	65.6	12.33	12.62
	2.0	36.2	6.80	36.6	6.87	6.84	61.6	11.59	58.4	10.98	11.40
	2.5	37.0	6.95	37.0	6.95	6.95	57.6	10.82	58.8	11.06	10.94
-0.07	1.5	36.2	6.80	35.6	6.69	6.74	65.4	12.29	65.0	12.21	12.25
	2.0	36.6	6.87	36.1	6.78	6.82	58.6	11.01	60.0	11.29	11.15
	2.5	36.6	6.87	36.4	6.84	6.86	58.0	10.90	54.0	10.15	10.52
-0.09	1.5	34.8	6.54	34.6	6.50	6.52	64.0	12.02	62.4	11.72	11.87
	2.0	35.6	6.70	35.8	6.72	6.71	59.2	11.12	61.6	11.59	11.36
	2.5	35.8	6.72	36.2	6.80	6.76	60.0	11.29	58.6	11.02	11.16
Fixed Fin		40.0	7.51	39.6	7.45	7.48	57.4	10.79	56.6	10.63	10.71

Note: Upper peak values of period measured between first and second maxima.

Lower peak values of period measured between first and second minima.

Upper peak values of time to double amplitude measured from amplitude at first maximum.

Lower peak values of time to double amplitude measured from amplitude at first maximum.

ndt signifies non-dimensional time, t/τ, as used on the computer and in the analysis.

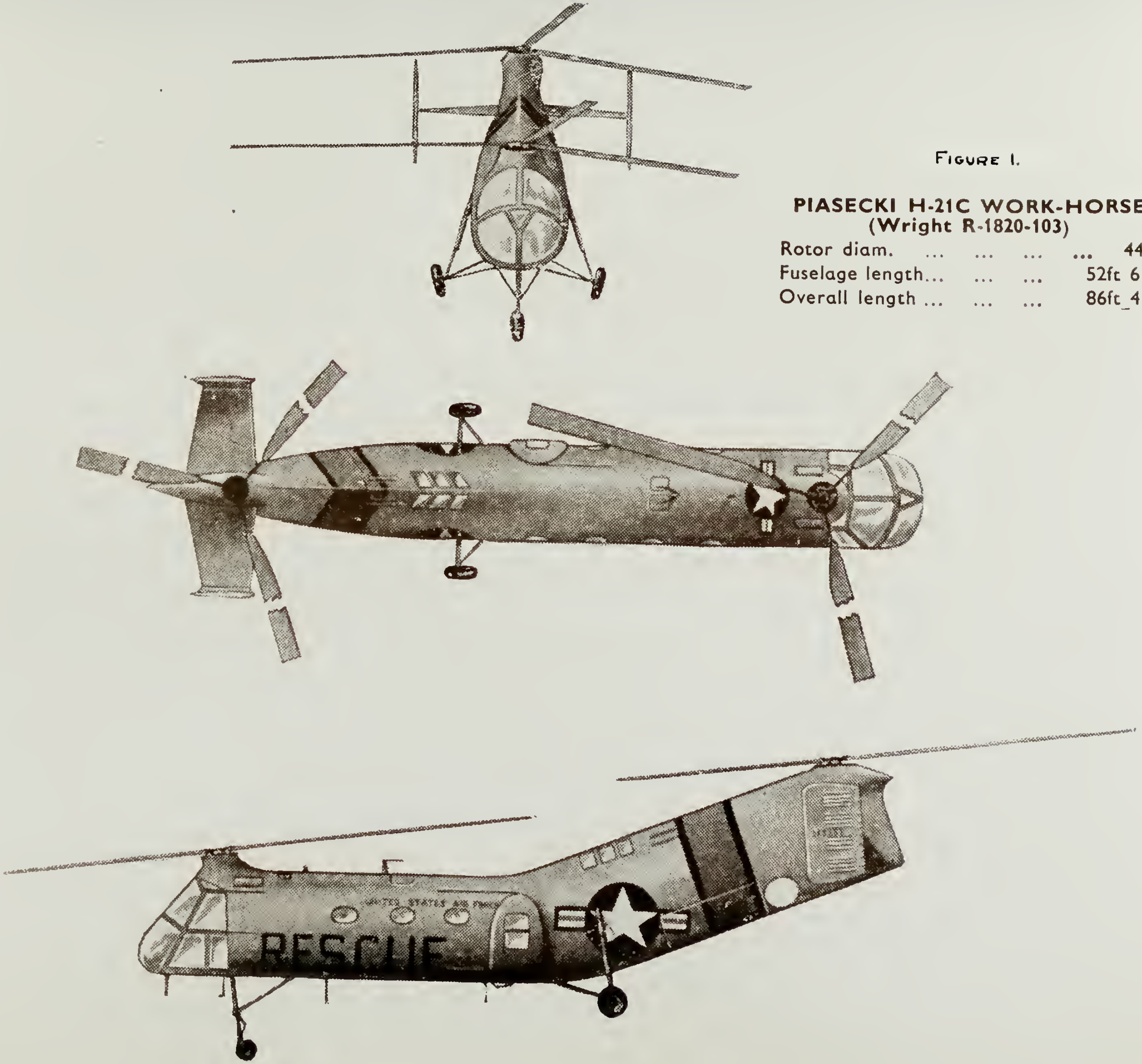

FIGURE I.

PIASECKI H-21C WORK-HORSE
(Wright R-1820-103)

Rotor diam.	44ft
Fuselage length	52ft 6in
Overall length	86ft 4in

FIG. 2

H-21 GEDA COMPUTER DIAGRAM

FLOATING VERTICAL TAIL FINS
CONTROLS FIXED
ONE INCH LATERAL CYCLIC DISPLACE AND HOLD CONTROL INPUT

SEA LEVEL
80 KNOTS

EQUATIONS:

Y: $-1.22\,D\beta_s = 0.0546\,\beta_s + 1.22\,D\Psi - 0.0546\,\Phi - C_1\delta_s - 0.000818$

L: $-0.0153\,D^2\Phi = 0.002245\,\beta_s - 0.00454\,D^2\Psi + 0.001961\,D\Psi + 0.00351\,D\Phi - C_2\delta_s - 0.0001798$

N: $-0.227\,D^2\Psi = -0.0020\,\beta_s + 0.0076\,D\Psi - 0.00454\,D^2\Phi - 0.00117\,D\Phi + C_3 D\delta_s + C_4\delta_s$

H: $-0.1985\,D^2\delta_s = -C_5\beta_s + C_6 D^2\Psi + C_7 D\Psi - C_8 D^2\Phi - C_9 D\Phi + C_{10}\Phi + C_{11} D\delta_s + C_{12}\delta_s$

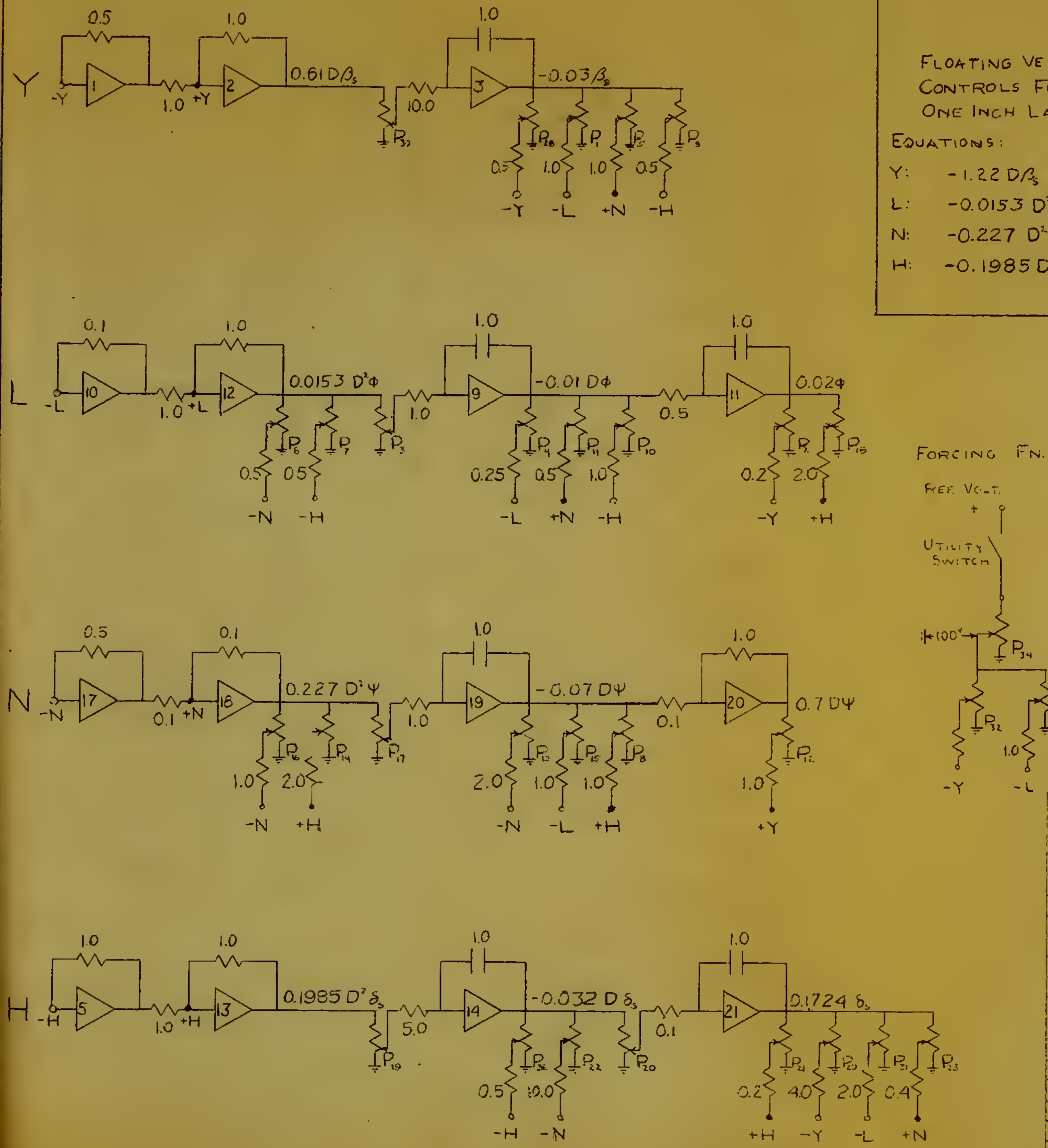

POT No.	VALUE OF COEFF. FOR P=1.0	VALUE DESIRED	POT. SETT'G, P
1	0.03	0.02245	.748
2	0.02	0.0109	.545
3	0.0153	0.01	.654
4	0.01	0.00878	.878
5	0.03	0.02	.667
6	0.0153	0.00454	.296
11	0.01	0.00587	.587
12	0.7	0.61	.871
13	0.07	0.0304	.435
15	0.07	0.0198	.283
16	0.227	0.0454	.2
17	0.227	0.07	.306
19	0.1985	0.16	.806
20	0.032	0.01724	.539
28	0.03	0.0273	.910
30	0.61	0.3	.492
32	100	81.6	.816
33	100	17.96	.150

POT No.	d₁	d₂	VALUE OF COEFF. FOR P=1.0	VALUE DESIRED	POT. SETT'G, P
7		0.145	0.0153	0.00835	.576
		0.125		0.007605	497
		0.105		0.0064	.418
		0.085		0.00516	.338
8	-0.03		0.07	0.0107	.153
	-0.05			0.0178	.255
	-0.07			0.025	.357
	-0.09			0.0322	.460
9	-0.03		0.03	0.0069	230
	-0.05			0.01145	382
	-0.07			0.16	.535
	-0.09			0.02065	.688
10	-0.03		0.01	0.00272	.272
	-0.05			0.00452	.452
	-0.07			0.00634	.634
	-0.09			0.00816	816

POT. No.	K	d₁	d₂	VALUE OF COEFF. FOR P=1.0	VALUE DESIRED	POT. SETT'G P
14			0.145	0.227	0.1388	.611
			0.125	↓	0.1196	.526
			0.105	↓	0.1008	.443
			0.085	↓	0.0814	.358
18			0.145	0.02	0.008	.4
			0.125	↓	0.00692	.346
			0.105	↓	0.00582	.291
			0.085	↓	0.0047	.235
21	1.5	-0.03		0.1724	0.0506	.293
		-0.05		↓	0.0472	.274
		-0.07		↓	0.0448	.260
		-0.09		↓	0.0418	.242
	2.0	-0.03		↓	0.0684	.396
		-0.05		↓	0.0650	.377
		-0.07		↓	0.0618	.358
		-0.09		↓	0.0584	.338
	2.5	-0.03		↓	0.0862	.5
		-0.05		↓	0.0826	.479
		-0.07		↓	0.0790	.458
		-0.09		↓	0.0750	.435
22	1.5			0.032	0.01342	.420
	2.0			↓	0.01412	.441
	2.5			↓	0.0149	.466
23	1.5			0.0862	0.01412	.164
	2.0			↓	0.01592	.185
	2.5			↓	0.01770	.205
29	1.5			0.0862	0.03036	.352
	2.0			↓	0.03406	.395
	2.5			↓	0.0378	.438
31	1.5			0.0862	0.01797	.206
	2.0			↓	0.0202	.234
	2.5			↓	0.0226	.262
36	1.5			0.032	0.02545	.796
	2.0			↓	0.02835	.885
	2.5			↓	0.0312	.975

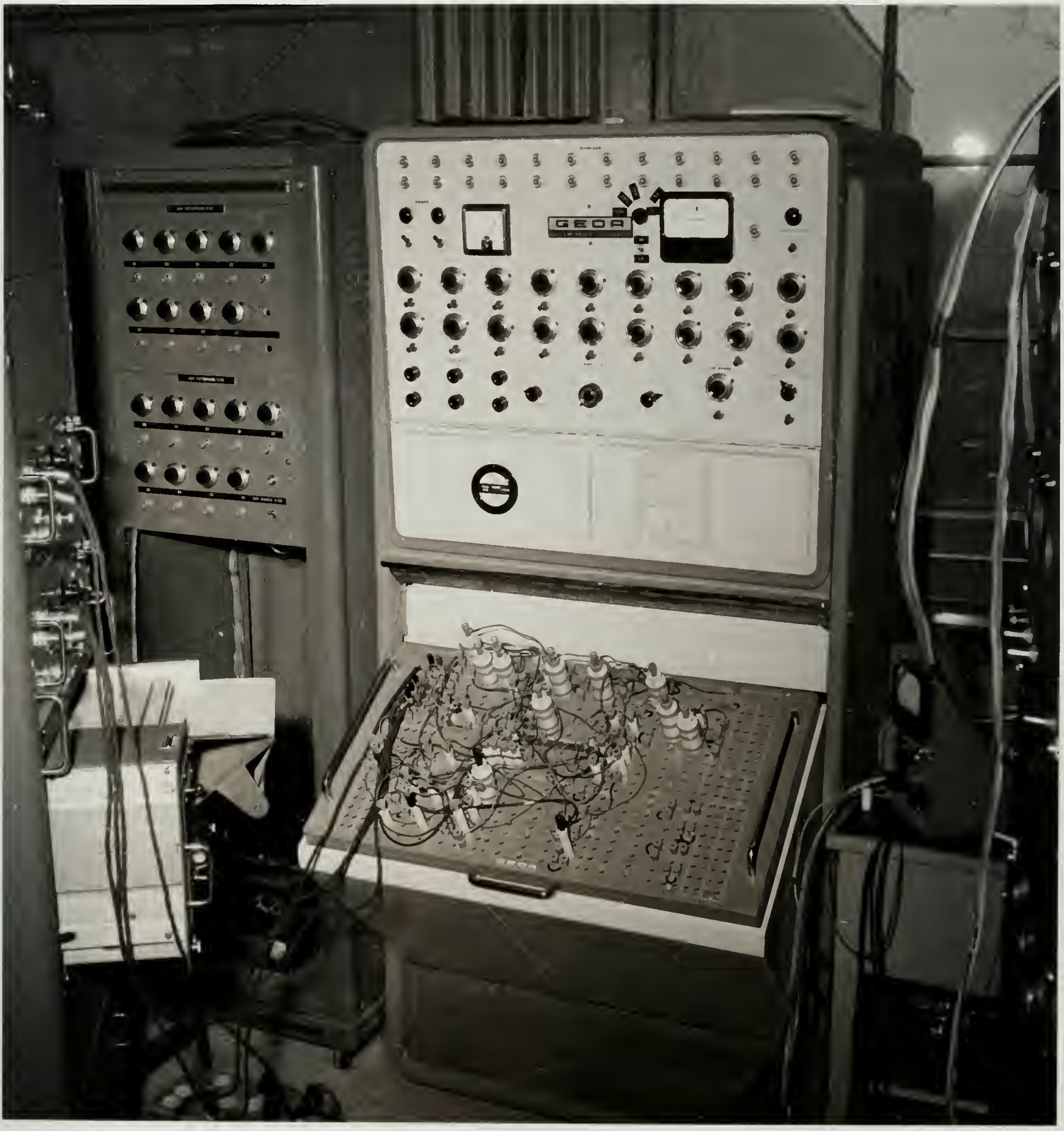

FIGURE 3.

L3 GEDA ANALOG COMPUTER

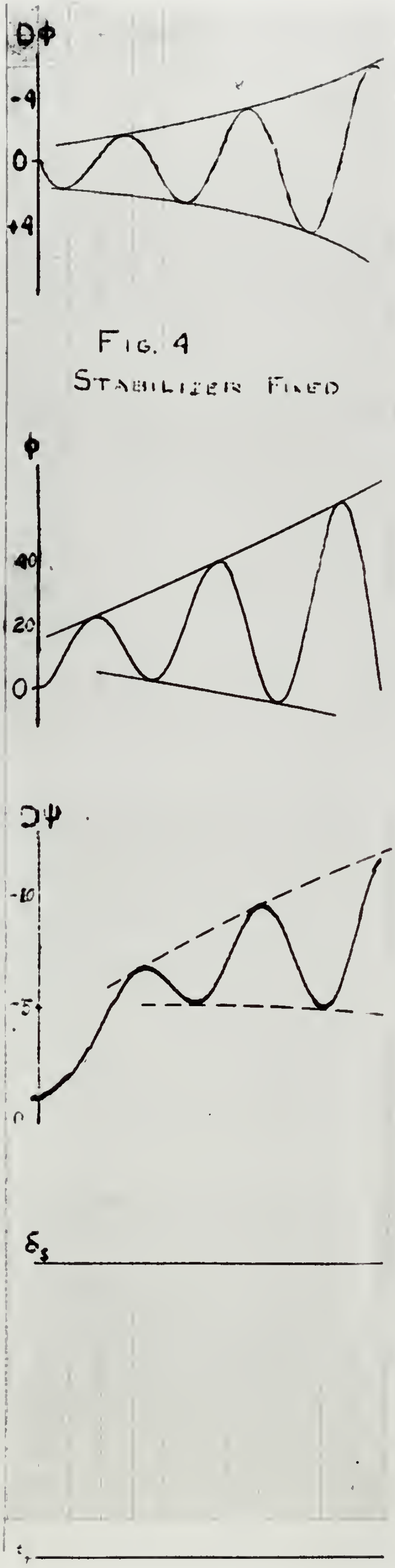

FIG. 4
STABILIZER FIXED

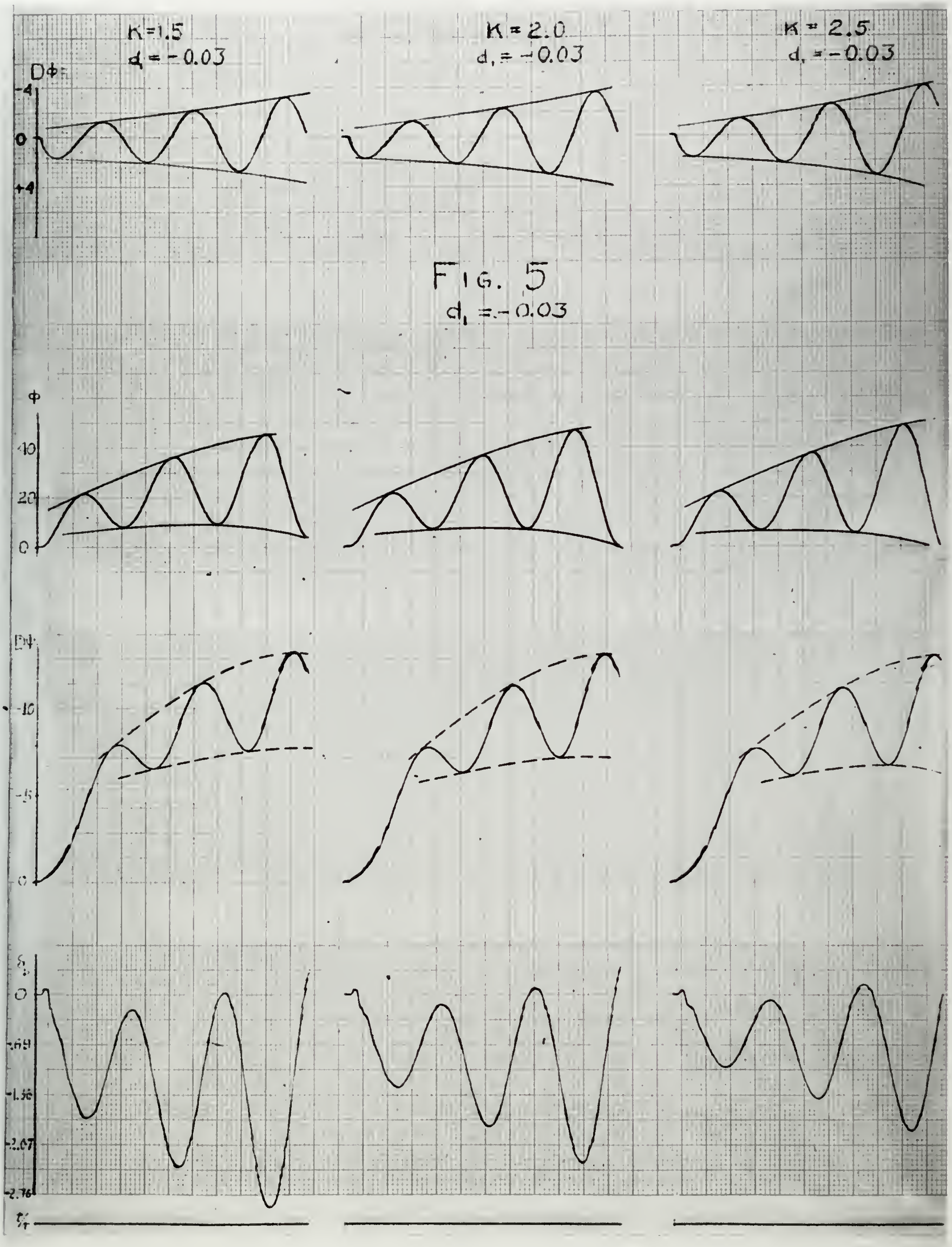
K=1.5
$d_1 = -0.03$
K = 2.0
$d_1 = -0.03$
K = 2.5
$d_1 = -0.03$
DΦ
-4
0
+4
Φ
40
20
0
DΨ
-10
-5
0
δ
0
-.69
-1.38
-2.07
-2.76
t/T

FIG. 5
$d_1 = -0.03$

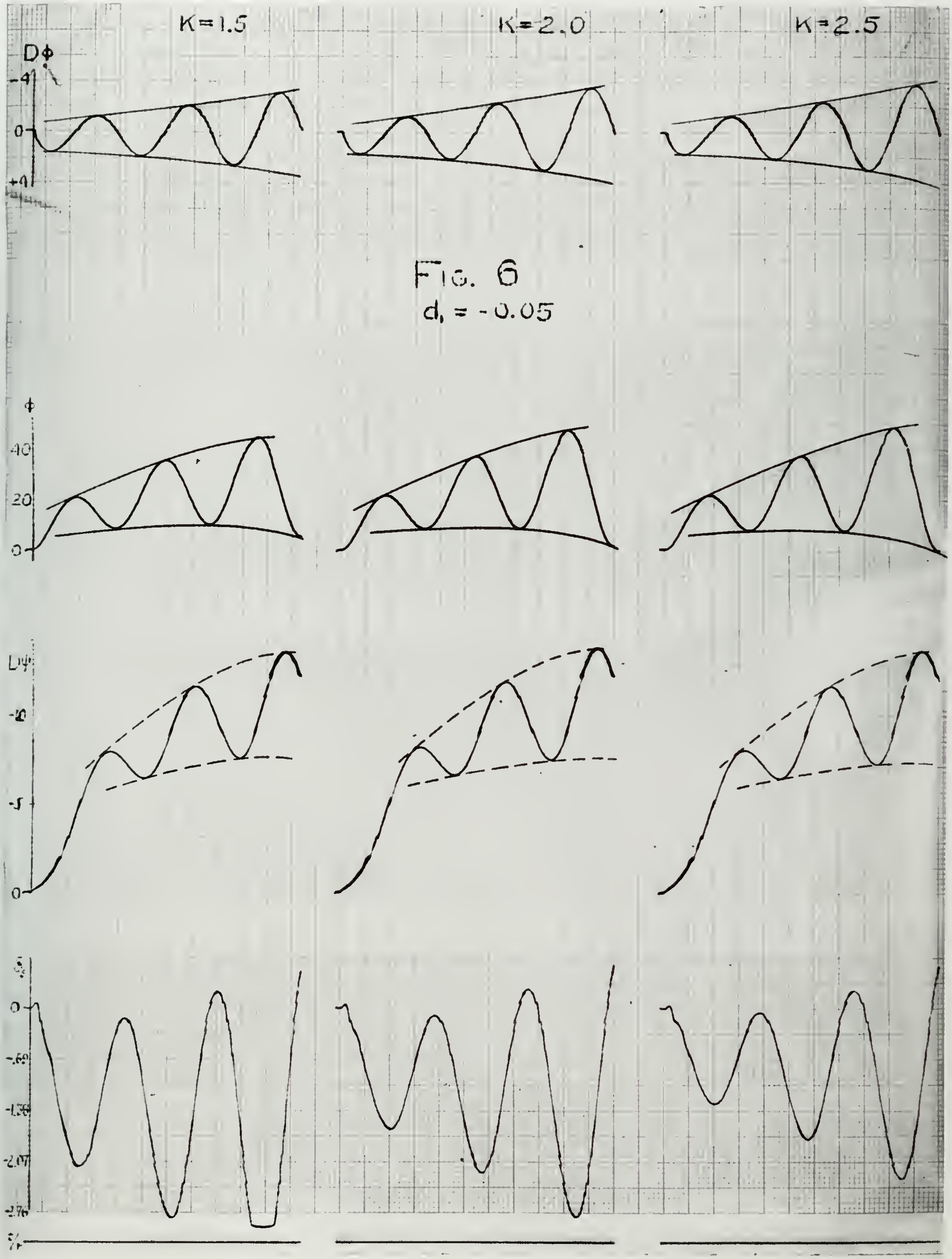

FIG. 6

$d_1 = -0.05$

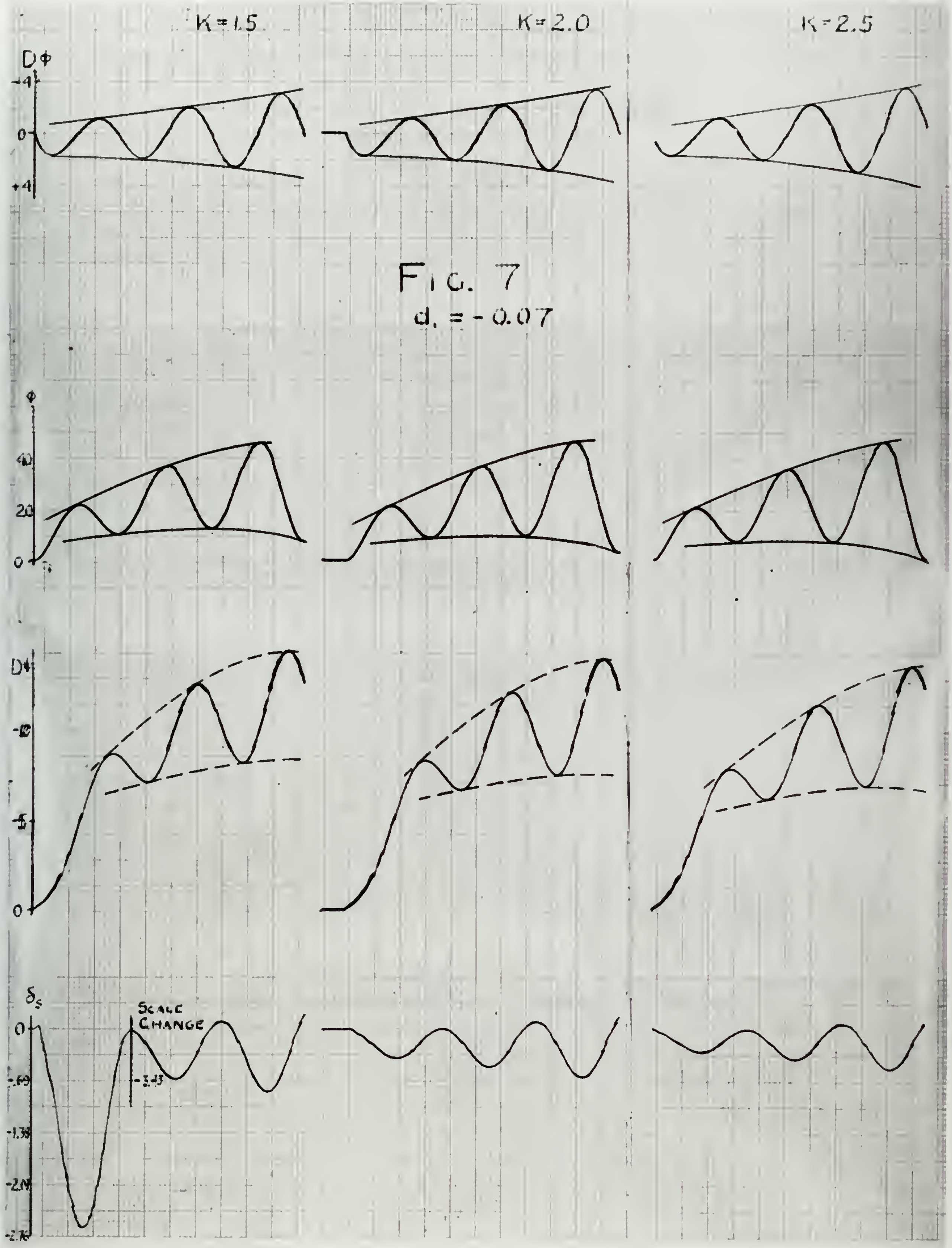
K=1.5
K=2.0
K=2.5
DΦ
-4
0
+4
Φ
40
20
0
DΨ
-10
-5
0
δs
0
-.69
-1.38
-2.07
-2.76
SCALE CHANGE
-3.45
t/T

FIG. 7
$d_1 = -0.07$

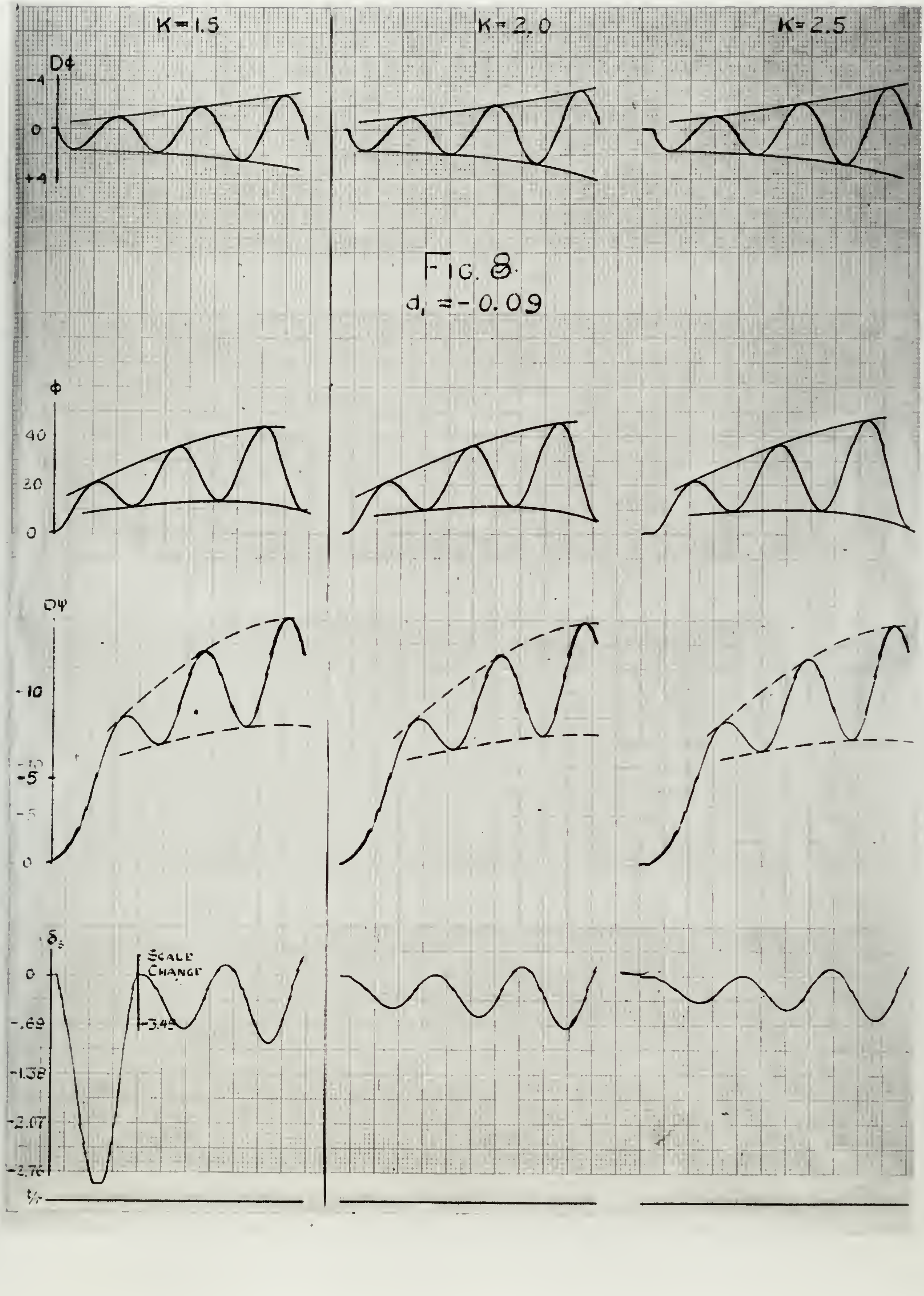
K=1.5
K=2.0
K=2.5
Dϕ
-4
0
+4
ϕ
40
20
0
Dψ
-10
-5
0
δs
0
-.69
-1.38
-2.07
-2.76
Scale Change
-3.45
t/τ

FIG. 8

$d_1 = -0.09$

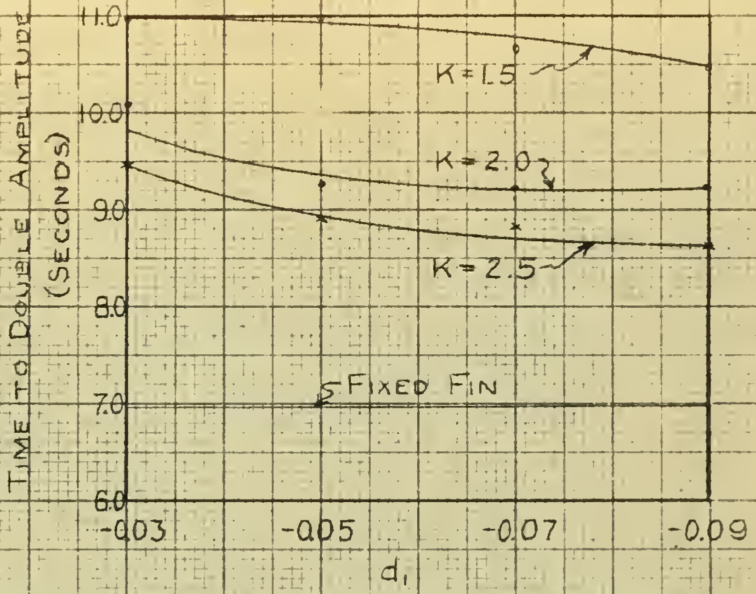

FIG. 9

EFFECT OF POSITION OF SUSPENSION POINT ON DAMPING (ROLL ANGLE)

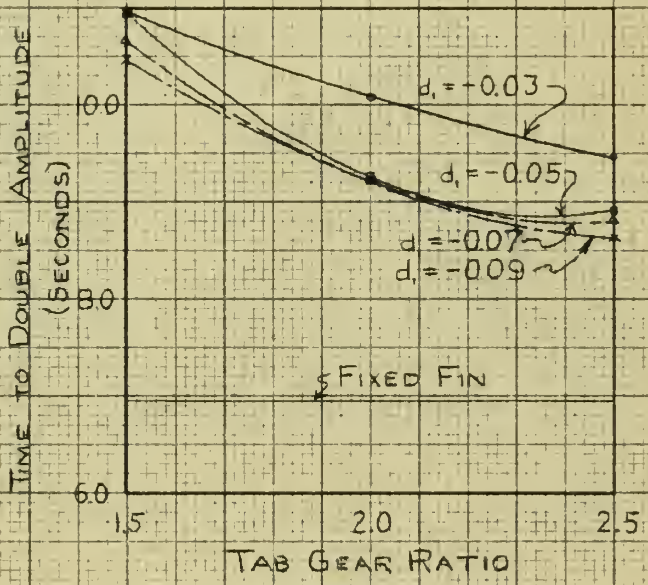

FIG. 10

EFFECT OF GEAR RATIO ON DAMPING

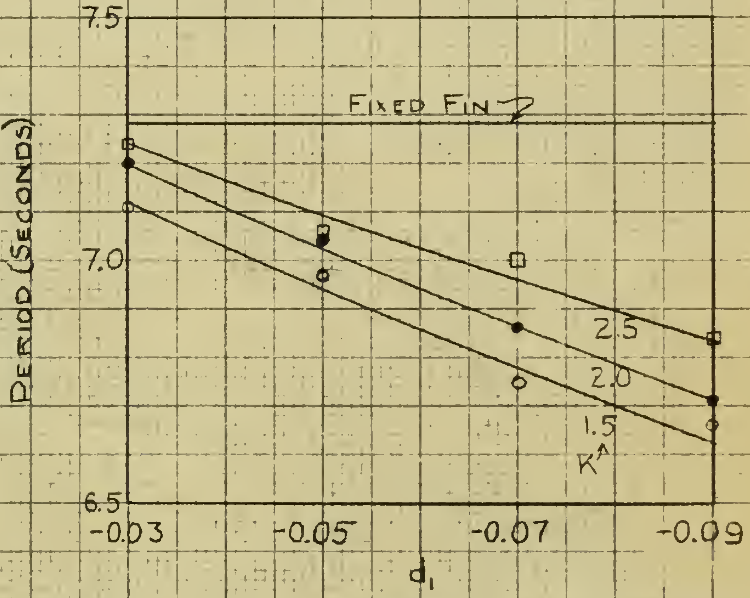

FIG. 11

EFFECT OF SUSPENSION POINT

ON PERIOD (ROLL ANGLE)

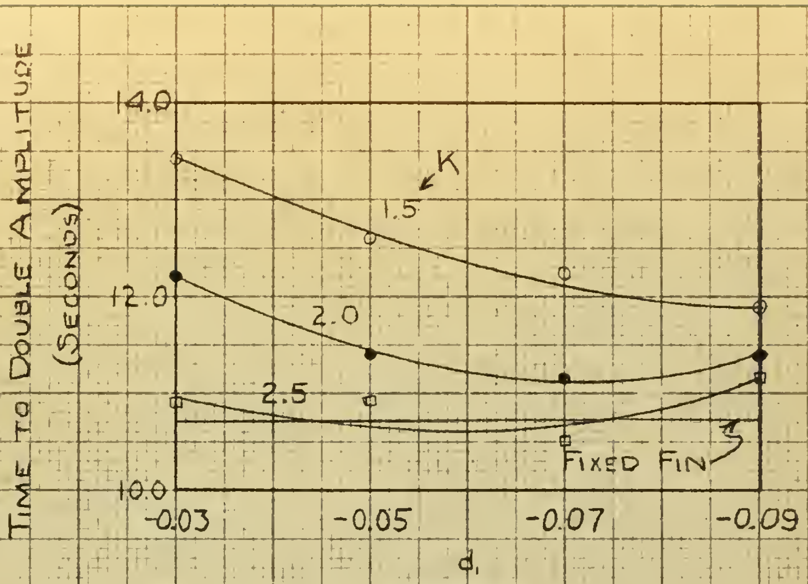

FIG. 12

EFFECT OF SUSPENSION POINT ON DAMPING

(ROLL RATE)

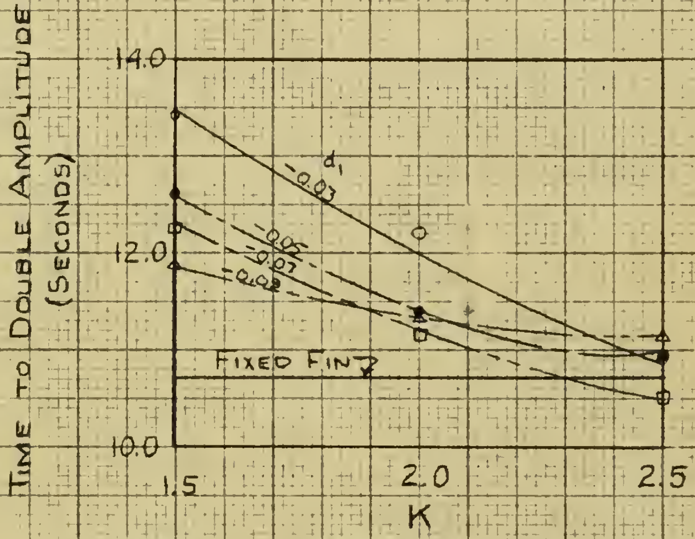

FIG. 13

EFFECT OF GEAR RATIO ON DAMPING

(ROLL RATE)

JA 17 58 BINDERY
4 APR 69 596

Thesis 35767
G57 Goodspeed
Control-fixed lateral
dynamic stability of the
H-21 helicopter ...

JA 17 58 BINDERY
4 APR 69 596

l
he
free-
l

Thesis 35767
G57 Goodspeed
Control-fixed lateral dynamic
stability of the H-21 helicopter
with free-floating vertical tail
fins.

thesG57
Control-fixed lateral dynamic stability
3 2768 002 13102 1
DUDLEY KNOX LIBRARY